4

Electric polarization

Clearly the electric polarization $\mathbf{P}$ of a crystalline insulator should be defined so as to carry the meaning of dipole moment per unit volume, but a precise formulation is surprisingly subtle. In Sec. 1.1 we briefly discussed the problems with a definition of $\mathbf{P}$ in terms of the (ionic plus electronic) charge density $\rho(\mathbf{r})$. These will be spelled out more fully in the next section, and in fact, we shall see that even a perfect knowledge of $\rho(\mathbf{r})$ is not enough, even in principle, to determine $\mathbf{P}$. As was strongly hinted in Ch. 1, a suitable definition can instead be given in terms of Berry phases, or equivalently, in terms of Wannier centers. This formulation will be developed in Secs. 4.2 and 4.3. In this way, a concept of bulk electric polarization is recovered, but only at the expense of abandoning a completely unique value of $\mathbf{P}$. Instead, we have to accept a definition that determines $\mathbf{P}$ only modulo a quantum $e\mathbf{R}/V_{\text{cell}}$, as in Eq. (1.7). The interpretation of this quantum will be discussed at some length in Sec. 4.4. The remaining sections will cover the relation of $\mathbf{P}$ to surface charges and the treatment of insulators in finite electric fields.

4.1 Statement of the problem

Let's imagine that we have a perfect knowledge of the charge density $\rho(\mathbf{r})$ in some insulating crystal. In the context of Ch. 2, this would take a form like

$$\rho(\mathbf{r}) = e \sum_{\mathbf{R}\boldsymbol{\tau}} Z_{\boldsymbol{\tau}}\, \delta^3(\mathbf{r} - \mathbf{R} - \boldsymbol{\tau}) - \frac{e}{(2\pi)^3} \sum_n \int_{\text{BZ}} |\psi_{n\mathbf{k}}(\mathbf{r})|^2 \, d^3k \qquad (4.1)$$

where the first term gives the nuclear contribution as a sum of delta functions at atom locations $\boldsymbol{\tau}$ in cell $\mathbf{R}$ (with $Z_{\boldsymbol{\tau}}$ the atomic number) and the second is the electronic contribution following from Eq. (2.36). It is natural to think that the electric polarization $\mathbf{P}$ can be expressed in terms of $\rho(\mathbf{r})$ in some

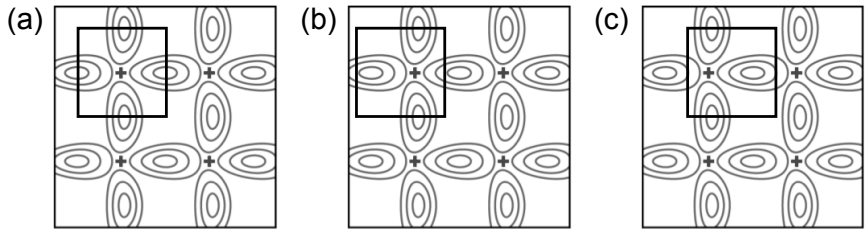

Figure 4.1 Model crystal with plus signs denoting delta-function nuclear charges and contours indicating electron clouds. The three panels indicate three different choices of unit cell boundaries (black squared), illustrating the dependence of Eq. (4.2) on unit cell location.

way, since it expresses a dipolar property and dipoles are normally defined in terms of charge densities. But any effort to do so quickly runs into problems.

One tempting but ultimately unsuccessful approach is to identify $\mathbf{P}$ with

$$\mathbf{P}_{\text{dip}} = \frac{1}{V_{\text{cell}}} \int_{\text{cell}} \mathbf{r}\, \rho(\mathbf{r})\, d^3r \tag{4.2}$$

where the integral represents the dipole moment of the charge distribution inside one unit cell. This was introduced as Eq. (1.1) in Sec. 1.1, but as mentioned there, it does not give a unique definition because of a dependence on the choice of unit cell. This is illustrated for a model crystal in Fig. 4.1. The result of evaluating Eq. (4.2) is evidently $P_x \equiv 0$ in Panel (a), while the cells in Panels (b) and (c) clearly contain dipoles pointing to the right and left ($P_x > 0$ and $P_x < 0$) respectively. If the crystal has an inversion or mirror symmetry, it may be possible to argue for a "most natural" choice of unit cell, but these are typically the cases where $\mathbf{P}$ vanishes anyway; we need an approach that works for cases with arbitrarily low symmetry. One clever suggestion could be to *average* over all possible unit cell locations, but unfortunately the result of this procedure this procedure is always exactly zero (see Ex. 4.1.1), which is hardly useful!

Another hint that this approach is not fruitful is to evaluate Eq. (4.2) for the case of, say, a silicon crystal polarized by an external electric field in the context of DFT calculations. It turns out that, no matter how the unit cell boundaries are chosen, the field-induced polarization change computed according to Eq. (4.2) is an order of magnitude too small to be consistent with the known dielectric response of Si as characterized by its dielectric constant $\epsilon \simeq 12$.

To understand why Eq. (4.2) fails, consider how $\mathbf{P}$ changes under a slow adiabatic change of the crystal Hamiltonian. We assume this Hamiltonian remains cell-periodic at all times, so that $\rho(\mathbf{r})$ and $\mathbf{j}(\mathbf{r})$ (the local microscopic

induced current density) also remain cell-periodic. But recall that in Ch. 1 we argued for an intimate relation between polarization and current in the form of Eq. (1.2) or (1.9), which says that the change in polarization $\delta\mathbf{P}$ after some infinitessimal time δt must be

$$\delta\mathbf{P} = \mathbf{J}\,\delta t \tag{4.3}$$

where

$$\mathbf{J}(t) = \frac{1}{V_{\text{cell}}}\int_{V_{\text{cell}}} \mathbf{j}(\mathbf{r},t)\,d^3r \tag{4.4}$$

is the adiabatically induced macroscopic current density expressed as a unit-cell average. Equation (4.4) has a formal similarity to Eq. (4.2), but there is an all-important difference in that Eq. (4.4) does *not* depend on the location of the cell boundary. This follows because $\mathbf{j}(\mathbf{r},t)$, unlike $\mathbf{r}\rho(r)$, remains a cell-periodic function of $\mathbf{r}$; the problematic position operator $\mathbf{r}$ is now absent, and the cell average is unambiguous.

Let's now see whether $\mathbf{P}_{\text{dip}}$ of Eq. (4.2) satisfies Eq. (4.3). We find

$$\begin{aligned}
\delta\mathbf{P}_{\text{dip}} &= \frac{1}{V_{\text{cell}}}\int_{V_{\text{cell}}} \mathbf{r}\,\delta\rho(\mathbf{r})\,d^3r \\
&= -\frac{\delta t}{V_{\text{cell}}}\int_{V_{\text{cell}}} \mathbf{r}\,[\nabla\cdot\mathbf{j}(\mathbf{r})]\,d^3r \\
&= \frac{\delta t}{V_{\text{cell}}}\left[\int_{V_{\text{cell}}} \mathbf{j}(\mathbf{r})\,d^3r - \int_{S_{\text{cell}}} \mathbf{r}\,(\mathbf{j}\cdot d\mathbf{S})\right]
\end{aligned} \tag{4.5}$$

where the divergence theorem $\dot\rho = -\nabla\cdot\mathbf{j}$ has been used in the form $\delta\rho(\mathbf{r}) = -\nabla\cdot\mathbf{j}(\mathbf{r})\,\delta t$ to express local charge conservation during the process. An integration by parts has been applied to get the last line, where the second term is a surface integral over the cell boundary S_{cell}. But the first term in this last line is nothing other than the true $\delta\mathbf{P}$, and moving the surface term to the other side of the equation we obtain

$$\delta\mathbf{P} = \delta\mathbf{P}_{\text{dip}} + \frac{\delta t}{V_{\text{cell}}}\int_{S_{\text{cell}}} \mathbf{r}\,(\mathbf{j}\cdot d\mathbf{S})\,. \tag{4.6}$$

Clearly $\delta\mathbf{P} \neq \delta\mathbf{P}_{\text{dip}}$, so that $\mathbf{P}_{\text{dip}}$ does not satisfy Eq. (4.3) and is therefore not valid, unless it can be shown that the surface term in Eq. (4.6) vanishes. But there is no reason why it should, in general. For a simple rectilinear $a\times b\times c$ unit cell, the change of the x-component of the polarization is just $(\delta t/bc)\int j_x\,dy\,dz$, where the integral is over the right side face of the unit cell. This extra term just measures *the current flowing through the face of the unit cell* during the adiabatic evolution, and in the silicon example mentioned above, is a much more important contribution than $\delta\mathbf{P}_{\text{dip}}$. In fact, there is

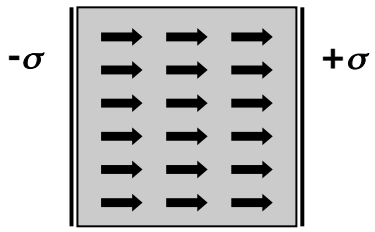

Figure 4.2 ...

no hope of extracting a knowledge of this current flow from the change of charge density $\delta\rho(\mathbf{r})$ alone.[1] This line of argument suggests that we must somehow go beyond a focus on charge densities, and consider currents, in order to arrive at a suitable definition of electric polarization.

Of course, if we have a knowledge of the charge density $\rho(\mathbf{r})$ everywhere in space for some finite crystallite, including at its surface, we could try to adopt the "thermodynamic limit" approach and let $\mathbf{P}$ be defined as the dipole per unit volume of this large crystallite in the limit that its size L goes to infinity. This approach only works, however, if the surface contributions can be shown to vanish in the thermodynamic limit. Unfortunately, this is not the case here, as illustrated in Fig. 4.2. Suppose that a crystallite of size $L \times L \times L$ is prepared under two different sets of conditions, such that the second set leads to the appearance of an extra surface charge density σ on the right side face and $-\sigma$ on the left. This extra charge density will make a contribution of $(L^2\sigma)(L)$ to the total dipole moment of the sample (charge on the surfaces times their separation); dividing by volume L^3, we see that the contamination of $\mathbf{P}$ by the surface contribution does not vanish in the thermodynamic limit. One could insist on choosing to define $\mathbf{P}$ in this way for a given crystallite with given surfaces, but a suitable bulk definition of $\mathbf{P}$ must depend on bulk properties alone.

If the information needed to compute $\mathbf{P}$ is not contained in the crystalline charge density $\rho(\mathbf{r})$, it seems very likely to be contained somehow in the underlying Bloch wavefunctions $\psi_{n\mathbf{k}}(\mathbf{r})$ from which $\rho(r)$ is constructed. For a finite system, such as a molecule or cluster, for which $\rho(\mathbf{r}) = -e\sum_j |\psi_j(\mathbf{r})|^2$, the electronic contribution to the dipole moment can be written in terms of expectation values of the position operator as $\int \mathbf{r}\,\rho(\mathbf{r})\,d^3r = -e\sum_j \langle\psi_j|\mathbf{r}|\psi_j\rangle$. Unfortunately, this kind of definition does not easily generalize to the crys-

[1] As an exception, note that if the crystal is actually composed of non-overlapping molecular entities such that $\rho(\mathbf{r})$ and $\mathbf{j}(\mathbf{r})$ vanish on the cell boundary, as in Fig. 1.1(a), then the troublesome surface term in Eq. (4.6) vanishes. It is only in this ideal Claussius-Mossotti context that $\mathbf{P}_{\text{dip}}$ can be accepted as a valid expression for the electric polarization.

talline case, where the expectation value $\langle\psi_{n\mathbf{k}}|\mathbf{r}|\psi_{n\mathbf{k}}\rangle = \int \mathbf{r}\,|\psi_{n\mathbf{k}}(\mathbf{r})|^2\,d^3r$ is ill-defined (the integrand blows up at $|\mathbf{r}| \to \infty$). This suggests that, if we are to base a theory of electric polarization on the Bloch functions $\psi_{n\mathbf{k}}(\mathbf{r})$, it should somehow depend not just on their magnitudes $|\psi_{n\mathbf{k}}|$, but perhaps on some phase property instead.

There is another problem with all of the definitions proposed above. Recall that in Sec. 1.1 we argued, on the basis of several different physical arguments, that $\mathbf{P}$ should only be well-defined modulo the quantum $e\mathbf{R}/V_{\text{cell}}$ of Eq. (1.7). Instead, all the above attempts at a definition lack this characteristic indeterminacy, and should be regarded with suspicion on this basis alone.

This is more or less how the situation stood in the computational electronic structure community in 1992. The problems with conventional attempts at a definition of electric polarization were understood, and various hints were perceived to be pointing in the direction of phase properties as the basis of a proper definition. The so-called "modern theory of polarization," based on developments of Resta (1992) and King-Smith and Vanderbilt (1993), was finally able to put the theory on a sound footing by making use of Berry-phase concepts, as we discuss next.

Exercise 4.1.1 Show that $\mathbf{P}_{\text{dip}}$ in Eq. (4.2) vanishes when averaged over all possible locations of the unit cell origin. Hint: First show that the average is proportional to

$$\int_{V_{\text{cell}}} \int_{V_{\text{cell}}} \mathbf{r}\,\rho(\mathbf{r}-\mathbf{r}')\,d^3r\,d^3r'$$

where $\mathbf{r}'$ is the shift of origin of the cell. Then focus on the $\mathbf{r}'$ integral and argue that the result vanishes.

4.2 Berry-phase theory of polarization

The essential problem with using a *static* dipole-moment-based approach to the definition of $\mathbf{P}$ is that attempts to average the static quantity $\mathbf{r}\rho(\mathbf{r})$ over a unit cell are doomed to failure, as this quantity is not a cell-periodic function. The difficulty arises from the appearance of the unbounded position operator $\mathbf{r}$ in the integrand $\mathbf{r}\rho(\mathbf{r})$. On the other hand, we introduced in Ch. 1 a *dynamic* definition of the *change* in electric polarization, Eq. (1.9), for a system undergoing some adiabatic evolution that preserves the crystal periodicity, such as a sublattice displacement or the application of some external field. In this case $\Delta\mathbf{P}$ is given as the time integral of the current $\mathbf{J}(t)$ that flows during the interval between the initial and final states of the evolving

system, as expressed in Eq. (1.9), with $\mathbf{J}$ understood to be the macroscopic average of the microscopic current density $\mathbf{j}(\mathbf{r})$ as expressed in Eq. (4.4). Here we set out to build a theory of polarization on this current-based view of the problem.

4.2.1 First-order change in polarization

As discussed in Sec. 1.1.2, for a system evolving adiabatically according to $H(\lambda)$ for some time-dependent $\lambda(t)$, we can related the current and polarization by

$$\mathbf{J} = \frac{d\mathbf{P}}{dt} = \frac{d\mathbf{P}}{d\lambda}\frac{d\lambda}{dt} = \dot{\lambda}\,\partial_\lambda \mathbf{P} \tag{4.7}$$

where $\partial_\lambda = d/d\lambda$. We shall first give a heuristic derivation of an expression for $\partial_\lambda \mathbf{P}$ using the methods of ordinary perturbation theory summarized in Sec. 2.3, and then follow with a more careful line of argument using the adiabatic perturbation theory of Sec. 3.3.

We consider a crystalline insulator as the Hamiltonian $H(\lambda)$ varies with some parameter λ that preserves the crystal periodicity, corresponding perhaps to a sublattice displacement or the application of some external field. We also focus as usual on the cell-periodic functions obeying $H_\mathbf{k}|u_{n\mathbf{k}}\rangle = E_{nk}|u_{n\mathbf{k}}\rangle$ with $H_\mathbf{k} = e^{-i\mathbf{k}\cdot\mathbf{r}} H e^{i\mathbf{k}\cdot\mathbf{r}}$ as in Sec. 2.1.5. Adapting the notation of Sec. 2.3 to this context, we define

$$\mathcal{Q}_\mathbf{k} = \sum_m^{\text{unocc}} |u_{m\mathbf{k}}\rangle\langle u_{m\mathbf{k}}| = 1 - \mathcal{P}_\mathbf{k} \tag{4.8}$$

where $\mathcal{P}_\mathbf{k} = \sum_n^{\text{occ}} |u_{n\mathbf{k}}\rangle\langle u_{n\mathbf{k}}|$ and

$$T_{n\mathbf{k}} = \sum_m^{\text{unocc}} \frac{|u_{m\mathbf{k}}\rangle\langle u_{m\mathbf{k}}|}{E_{n\mathbf{k}} - E_{m\mathbf{k}}}\,. \tag{4.9}$$

Then the first-order change in an occupied-state wavefunction $|u_{n\mathbf{k}}\rangle$ with the perturbation $\partial_\lambda H_\mathbf{k}$ in Eq. (2.81) becomes

$$\mathcal{Q}_\mathbf{k}\,|\partial_\lambda u_{n\mathbf{k}}\rangle = T_{n\mathbf{k}}\,(\partial_\lambda H_\mathbf{k})\,|u_{n\mathbf{k}}\rangle \tag{4.10}$$

and it's contribution to the change in the expectation value of operator $\mathcal{O}$, Eq. (2.85), is now

$$\partial_\lambda \langle\mathcal{O}\rangle_{n\mathbf{k}} = 2\text{Re}\,\langle u_{n\mathbf{k}}|\mathcal{O}\mathcal{Q}_\mathbf{k}|\partial_\lambda u_{n\mathbf{k}}\rangle\,. \tag{4.11}$$

Summing over all the occupied bands $|u_{n\mathbf{k}}\rangle$ and reversing the order of the

matrix element, the total change is, in view of Eq. (2.33),

$$\partial_\lambda \langle \mathcal{O} \rangle = \frac{V_{\text{cell}}}{(2\pi)^3} \sum_n^{\text{occ}} \int_{\text{BZ}} 2\text{Re} \, \langle \partial_\lambda u_{n\mathbf{k}} | \mathcal{Q}_\mathbf{k} \mathcal{O} | u_{n\mathbf{k}} \rangle \, d^3k \,. \tag{4.12}$$

Now formally, the electric polarization should be dipole moment per unit volume, or $-e\langle \mathbf{r} \rangle / V_{\text{cell}}$, so ideally we should like to replace $\mathcal{O}$ with $\mathbf{r}$ in Eq. (4.12). Is this permissible? From Eq. (4.8) we see that this would involve matrix elements of the form $\langle u_{m\mathbf{k}} | \mathbf{r} | u_{n\mathbf{k}} \rangle$ between *different* Bloch states $|u_{m\mathbf{k}}\rangle$ (empty) and $|u_{n\mathbf{k}}\rangle$ (occupied). We saw previously that *diagonal* matrix elements of the form $\langle u_{n\mathbf{k}} | \mathbf{r} | u_{n\mathbf{k}} \rangle$ are ill-defined for the position operator, but what we can argue that *off-diagonal* ones *are* well defined, using a trick involving the velocity operator.

Recall from Sec. 2.1.5 that the velocity operator is properly defined as

$$\mathbf{v} = \frac{-i}{\hbar} [\mathbf{r}, H] \tag{4.13}$$

from which it follows that $\mathbf{v}_\mathbf{k} = e^{-i\mathbf{k}\cdot\mathbf{r}} \mathbf{v} e^{i\mathbf{k}\cdot\mathbf{r}}$ is

$$\mathbf{v}_\mathbf{k} = (-i/\hbar)[\mathbf{r}, H_\mathbf{k}] \tag{4.14}$$

(since $\mathbf{r}$ commutes with $e^{i\mathbf{k}\cdot\mathbf{r}}$). For a simple Hamiltonian of the form $H = p^2/2m + V(\mathbf{r})$ the velocity operator is just $\mathbf{v} = \mathbf{p}/m$, where m is the electron mass; this simplified expression often appears in the literature. However, we will adopt the proper expression in terms of the commutator above, in part because it must be used in more complicated cases, as when spin-orbit coupling or external fields are present as discussed in Sec. 2.1.2. More importantly, however, it is necessary to use this form in the next steps of our derivation. Starting from Eq. (4.14) and using the identity $\langle u_{m\mathbf{k}} | [\mathbf{r}, H_\mathbf{k} | u_{n\mathbf{k}} \rangle = (E_{n\mathbf{k}} - E_{m\mathbf{k}}) \langle u_{m\mathbf{k}} | \mathbf{r} | u_{n\mathbf{k}} \rangle$, we find that

$$\langle u_{m\mathbf{k}} | \mathbf{r} | u_{n\mathbf{k}} \rangle = i\hbar \, \frac{\langle u_{m\mathbf{k}} | \mathbf{v}_\mathbf{k} | u_{n\mathbf{k}} \rangle}{E_{n\mathbf{k}} - E_{m\mathbf{k}}} \,. \tag{4.15}$$

We appear to have tamed the unruly position operator appearing on the left-hand side above! After all, the matrix elements of the velocity operator, which is just $\mathbf{p}/m$ in simple cases, are perfectly well defined. However, it is crucial to keep in mind that Eq. (4.15) only holds when $|u_{n\mathbf{k}}\rangle$ and $|u_{m\mathbf{k}}\rangle$ are both eigenstates of $H_\mathbf{k}$, not for any arbitrary states of Bloch form, and only when $m \neq n$, as when n and m are occupied and empty respectively. When $\mathbf{v} = \mathbf{p}/m$ this equation takes the familiar form[2] $\langle u_{m\mathbf{k}} | \mathbf{r} | u_{n\mathbf{k}} \rangle = (-i/m\omega_{mn,\mathbf{k}}) \langle u_{m\mathbf{k}} | \mathbf{p} | u_{n\mathbf{k}} \rangle$, where $\hbar\omega_{mn,\mathbf{k}} = E_{m\mathbf{k}} - E_{n\mathbf{k}}$, which

[2] See Ex. 4.2.1

often appears in solid state physics texts, as for example in the discussion of the equivalence between expressions based on $\mathbf{r}$ or $\mathbf{p}$ for the optical dipole matrix element.

Multiplying both sides of Eq. (4.15) on the left by $|u_{m\mathbf{k}}\rangle$ and summing over all unoccupied bands m then yields

$$\mathcal{Q}_{\mathbf{k}}\,\mathbf{r}\,|u_{n\mathbf{k}}\rangle = i\hbar\,T_{n\mathbf{k}}\,\mathbf{v}_{\mathbf{k}}\,|u_{n\mathbf{k}}\rangle\,. \tag{4.16}$$

Inserting this in Eq. (4.12) with the heuristic identification $\mathbf{P} = -e\langle\mathbf{r}\rangle/V_{\text{cell}}$, we find the important result

$$\partial_\lambda \mathbf{P} = \frac{e\hbar}{(2\pi)^3}\sum_n^{\text{occ}}\int_{\text{BZ}} 2\text{Im}\,\langle\partial_\lambda u_{n\mathbf{k}}|T_{n\mathbf{k}}\mathbf{v}_{\mathbf{k}}|u_{n\mathbf{k}}\rangle\,d^3k\,. \tag{4.17}$$

Using Eq. (4.10) this can also be written as

$$\partial_\lambda \mathbf{P} = \frac{e\hbar}{(2\pi)^3}\sum_n^{\text{occ}}\int_{\text{BZ}} 2\text{Im}\,\langle u_{n\mathbf{k}}|(\partial_\lambda H_{\mathbf{k}})T^2_{n\mathbf{k}}\mathbf{v}_{\mathbf{k}}|u_{n\mathbf{k}}\rangle\,d^3k \tag{4.18}$$

involving energy denominators squared. These equations give the first-order change of polarization with respect to some perturbation λ.

Formulas like these have formed the basis for the computation of polarization responses in solids that was developed in the 1980's (see, e.g., Littlewood, 1980; Baroni and Resta, 1986; Baroni et al., 1987), drawing on the early formulation of Pick et al. (1970). These methods are nicely reviewed in Baroni et al. (2001) and in the pair of papers by Gonze (1997) and Gonze and Lee (1997). Two important examples of polarization responses that can be computed using these methods are the Born or dynamical effective charge tensor

$$Z^*_{\alpha,s\mu} = \frac{\partial P_\alpha}{\partial R_{s\mu}} \tag{4.19}$$

describing the polarization in direction α induced by a sublattice displacement of atom s in direction μ, and the piezoelectric tensor

$$c_{\alpha,\mu\nu} = \frac{\partial P_\alpha}{\partial \eta_{\mu\nu}} \tag{4.20}$$

describing the corresponding derivative with respect to a strain $\eta_{\mu\nu}$. Similar methods can be used to treat perturbations of other operators arising from a first-order applied electric field $\boldsymbol{\mathcal{E}}$. Since the field enters the Hamiltonian in the form $e\boldsymbol{\mathcal{E}}\cdot\mathbf{r}$, this involves solving for the field derivative of $|u_{n\mathbf{k}}\rangle$ using Eq. (4.10) in the form

$$\mathcal{Q}_{\mathbf{k}}|\partial_\lambda u_{n\mathbf{k}}\rangle = e\,T_{n\mathbf{k}}\,\mathbf{r}\,|u_{n\mathbf{k}}\rangle\,, \tag{4.21}$$

where the problematic position operator on the right-hand side can again be tamed using Eq. (4.15). This approach can even be used to compute the electric susceptibility

$$\chi_{\mu\nu} = \frac{\partial P_\mu}{\partial \mathcal{E}_\nu} = \frac{e^2\hbar}{(2\pi)^3} \sum_n^{\text{occ}} \int_{\text{BZ}} 2\text{Re}\,\langle u_{n\mathbf{k}}|v_{\mathbf{k},\mu} T^3_{n\mathbf{k}} v_{\mathbf{k},\nu}|u_{n\mathbf{k}}\rangle\, d^3k\,. \tag{4.22}$$

In practice the sums over unoccupied states are usually eliminated by replacing the formal Eqs. (4.10) and (4.21) with an iterative solution of a Sternheimer equation taking the form of Eq. (2.76).

Some readers may be concerned about whether the left-hand side of Eq. (4.15) is even well-defined, or about whether the heuristic identification of $\mathbf{P}$ with $e\mathbf{r}/V_{\text{cell}}$ even makes sense in an infinite crystal. We can confirm that the results derived above are correct in a more convincing way by abandoning a purely static view of the perturbation, and returning to the adiabatic perturbation theory derived in Sec. 3.3. There we found that the instantaneous wavefunction at time t has a first-order correction proportional to $\dot\lambda$, as in Eq. (3.50). Translating Eq. (3.52) into the present context of a crystalline solid, the first-order-in-$\dot\lambda$ correction to each occupied Bloch function is given by

$$|\delta u_{n\mathbf{k}}\rangle = -i\hbar T_{n\mathbf{k}} |\partial_\lambda u_{n\mathbf{k}}\rangle \tag{4.23}$$

respectively. The $|u_{n\mathbf{k}}\rangle$ are normalized to the unit cell of volume V_{cell}, so the induced response from a single Bloch state is

$$\begin{aligned} \langle \mathcal{O}\rangle_{n\mathbf{k}}/\dot\lambda &= 2\text{Re}\,\langle u_{n\mathbf{k}}|\mathcal{O}|\delta u_{n\mathbf{k}}\rangle \\ &= 2i\hbar\,\text{Im}\,\langle \partial_\lambda u_{n\mathbf{k}}|T_{n\mathbf{k}}\mathcal{O}|u_{n\mathbf{k}}\rangle \end{aligned} \tag{4.24}$$

where we substituted Eq. (4.23) and reversed the matrix element to get the second line. Specializing $\mathcal{O}$ now to the current operator $\boldsymbol{\mathcal{J}} = -e\mathbf{v}$ and summing over all occupied bands, the total induced current is[3]

$$\mathbf{J}/\dot\lambda = \frac{e\hbar}{(2\pi)^3} \sum_n \int_{\text{BZ}} 2\text{Im}\,\langle \partial_\lambda u_{n\mathbf{k}}|T_{n\mathbf{k}}\mathbf{v}_k|u_{n\mathbf{k}}\rangle\, d^3k\,, \tag{4.25}$$

The left-hand side is just $(d\mathbf{P}/dt)/(d\lambda/dt) = d\mathbf{P}/d\lambda = \partial_\lambda \mathbf{P}$, confirming the result presented earlier in Eq. (4.17) that was derived using a less rigorous argument. Similarly, the response to an $\mathcal{E}$-field perturbation in Eqs. (4.21-4.22) can be rederived by other methods, as by treating $\boldsymbol{\mathcal{E}}$ as arising from a vector potential $\mathbf{A}(t) = -c\boldsymbol{\mathcal{E}}t$ increasing linearly in time and again applying the methods of adiabatic perturbation theory.

[3] Note that the definitions of $\boldsymbol{\mathcal{J}}$ and $\mathbf{J} = \langle \boldsymbol{\mathcal{J}}\rangle/V_{\text{cell}}$ differ by a factor of V_{cell}.

4.2.2 Change of polarization on an adiabatic path

At this point, we find ourselves in a strange situation. We have derived Eqs. (4.17-4.18) expressing the *derivatives* of the polarization with respect to various perturbations such as sublattice displacements or external fields. On the other hand, we still have no formal expression for the *polarization itself*. Usually one expects that the computation of the derivative of some object is should be more difficult than the computation of the object itself. In the early 1990s, however, the electronic structure community found itself in the strange position of being able to calculate derivatives of $\mathbf{P}$, but not $\mathbf{P}$ itself. This paradoxical situation was resolved with the arrival of the "modern theory of polarization" based on Berry phases in the early 1990s. We are finally now ready to develop this theory.

To do so, we follow Resta (1992) and temporarily avoid the question of defining $\mathbf{P}$ itself and focus instead on the *change* of $\mathbf{P}$ during an adiabatic evolution of the system from some initial configuration i to a final one f, as in Eq. (1.13), which we repeat here:

$$\Delta\mathbf{P}_{\mathrm{i}\to\mathrm{f}} = \int_{\mathrm{i}}^{\mathrm{f}} \left(\frac{d\mathbf{P}}{d\lambda}\right) d\lambda \,. \tag{4.26}$$

Since we have well-defined formulas such as Eqs. (4.17) and (4.18) for the derivative appearing above, it should be possible to calculate the polarization change in practice by numerically integrating Eq. (4.26) on a mesh of λ values connecting λ_i to λ_f. For example, to compute the spontaneous polarization $\mathbf{P}_{\mathrm{s}}$ in a ferroelectric material such as $PbTiO_3$, one can let λ_i and λ_f refer to the centrosymmetric cubic structure and the ground-state ferroelectric structure respectively, and let λ linearly interpolate between them. Since we expect the polarization to vanish in the centrosymmetric initial configuration, we can then identify $\Delta\mathbf{P}$ with $\mathbf{P}_{\mathrm{s}}$. In practice, choosing only a few mesh points in λ often provides adequate convergence.

In one sense, Resta's numerical integration algorithm solves the problem of computing $\mathbf{P}$ in polar insulators. However, it is less than satisfactory on two counts. On the practical side, the calculation is tedious, requiring the construction of a path connecting the system of interest to a nonpolar reference configuration, checking that the system remains insulating along this path, and then carrying out the somewhat heavy linear-response calculation of the polarization derivative at each intermediate configuration. And on the philosophical side, it begs a number of questions: Is the construction of an intermediate path really necessary? If one were to choose two different paths leading from i to f, would Eq. (4.26) give the same answer, independent of path? If so, shouldn't it be possible to replace the formulation of Eq. (4.26)

with one that only requires a pair of calculations, one at the initial and one at the final configuration?

We discussed related questions in some detail in Sec. 1.1, where we gave arguments that the change in polarization should be the same modulo a quantum for two paths connecting the same states as in Fig. 1.5(a), or zero modulo a quantum for a closed path as in Fig. 1.5(b). Other arguments given later in Ch. 1 reinforced this hypothesis. But can we show mathematically that it should be so? To do this, we return to Eq. (4.17), now leaving computational questions aside for the moment, and concentrating instead on formal developments by which we can manipulate Eq. (4.17) into a path-independent form.

To do so we make use of another trick involving the velocity operator, namely the simple identity

$$\partial_{\mathbf{k}} H_{\mathbf{k}} = \hbar \mathbf{v}_{\mathbf{k}} \,. \tag{4.27}$$

whose proof follows directly by taking the $\mathbf{k}$-derivative[4] of $H_{\mathbf{k}}$ as defined in Eq. (2.39) (see also Ex. 2.1.1). But note that if we apply Eq. (4.10) to find the first $\mathbf{k}$-derivative of the Bloch function $|u_{n\mathbf{k}}\rangle$ and substitute Eq. (4.27), we get

$$\mathcal{Q}_{\mathbf{k}} \, |\partial_{\mathbf{k}} u_{n\mathbf{k}}\rangle = \hbar \, T_{n\mathbf{k}} \, v_{\mathbf{k}} \, |u_{n\mathbf{k}}\rangle \,. \tag{4.28}$$

Incidentally, combining this with Eq. (4.16) yields the remarkably simple relation $\mathcal{Q}_{\mathbf{k}} \, \mathbf{r} \, |u_{n\mathbf{k}}\rangle = i \, \mathcal{Q}_{\mathbf{k}} \, |\partial_{\mathbf{k}} u_{n\mathbf{k}}\rangle$, suggesting the heuristic replacement

$$\mathbf{r} \;\longrightarrow\; i\partial_{\mathbf{k}} \tag{4.29}$$

(compare $\mathbf{p} \to -i\hbar\partial_{\mathbf{r}}$ in quantum mechanics) which can sometimes be used as a shortcut in derivations. However, our goal here is to substitute Eq. (4.28) into Eq. (4.17) to eliminate $\mathbf{v}_{\mathbf{k}}$. Remarkably, this also eliminates the sum over unoccupied states entirely, and Eq. (4.17) becomes

$$\partial_\lambda \mathbf{P} = \frac{e}{(2\pi)^3} \sum_n^{\text{occ}} \int_{\text{BZ}} 2\text{Im} \, \langle \partial_\lambda u_{n\mathbf{k}} | \mathcal{Q}_{\mathbf{k}} | \partial_{\mathbf{k}} u_{n\mathbf{k}} \rangle \, d^3k \,. \tag{4.30}$$

It is not hard to show that $\sum_n^{\text{occ}} \langle \partial_\lambda u_{n\mathbf{k}} | \mathcal{P}_{\mathbf{k}} | \partial_{\mathbf{k}} u_{n\mathbf{k}} \rangle$ is pure real (see Ex. 4.2.2), so using $\mathcal{Q}_{\mathbf{k}} = 1 - \mathcal{P}_{\mathbf{k}}$ this can be written more concisely as

$$\partial_\lambda \mathbf{P} = \frac{e}{(2\pi)^3} \sum_n^{\text{occ}} \int_{\text{BZ}} 2\text{Im} \, \langle \partial_\lambda u_{n\mathbf{k}} | \partial_{\mathbf{k}} u_{n\mathbf{k}} \rangle \, d^3k \,. \tag{4.31}$$

The disappearance of the sum over unoccupied states embodied in the $T_{n\mathbf{k}}$

[4] We use the notations $\partial_{\mathbf{k}}$ and $\nabla_{\mathbf{k}}$ interchangeably. The form $\partial_{\mathbf{k}}$ is used here for for consistency with other perturbations ∂_λ.

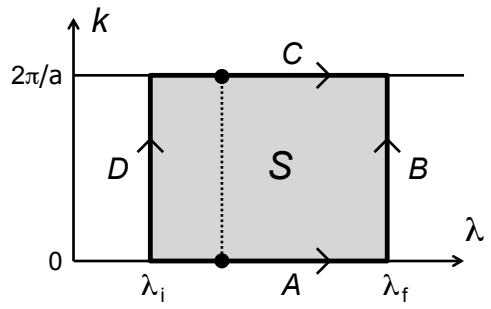

Figure 4.3 Region of integration of Berry curvature $\Omega_n^{(\lambda k)}$ in Eq. (4.35). A positive sense of circulation around the boundary traces segments A and B as drawn and C and D in reverse.

operator is very encouraging. After all, we expect the electric polarization to be a ground-state property, and as such, we expect it to depend only on the occupied Bloch states $|u_{n\mathbf{k}}\rangle$. This is manifestly true of ordinary observables, for which the expectation value per unit cell is.

$$\langle \mathcal{O} \rangle_{\text{cell}} = \frac{1}{(2\pi)^3} \sum_n^{\text{occ}} \int_{\text{BZ}} \langle u_{n\mathbf{k}} | \mathcal{O} | u_{n\mathbf{k}} \rangle \, d^3k \,. \tag{4.32}$$

Equation (4.31) is not of this form, but having lost the problematic sum over unoccupied states, it is much closer to Eq. (4.32) than was Eq. (4.17).

There is another remarkable aspect of Eq. (4.31): its integrand takes the form of a Berry curvature! Compare, for example, with Eq. (3.31) in Sec. 3.2.1. To develop this connection, let's restrict our attention for the moment to the case of a single occupied band n in a 1D insulator of lattice constant a. Translating Eq. (4.31) to this context, the contribution P_n from this band obeys

$$\partial_\lambda P_n = \frac{e}{2\pi} \int_0^{2\pi/a} 2\text{Im} \, \langle \partial_\lambda u_{nk} | \partial_k u_{nk} \rangle \, dk \,. \tag{4.33}$$

It is then natural to regard (λ, k) as defining a 2D parameter space in which we define Berry potentials $A_n^{(\lambda)} = i\langle u_{nk} | \partial_\lambda u_{nk} \rangle$ and $A_n^{(k)} = i\langle u_{nk} | \partial_k u_{nk} \rangle$ and the Berry curvature $\Omega_n^{(\lambda k)} = -2\text{Im} \, \langle \partial_\lambda u_{nk} | \partial_k u_{nk} \rangle$. Then Eq. (4.33) reduces to the marvelously simple form

$$\partial_\lambda P_n = \frac{-e}{2\pi} \int_0^{2\pi/a} \Omega_n^{(\lambda k)} \, dk \,. \tag{4.34}$$

That is, the first-order change in polarization is just proportional to the BZ integral of the Berry curvature in (λ, k) space!

The next step is to insert this into Eq. (4.26) to compute the contribution

$\Delta P_{n,\mathrm{if}}$ to the change in polarization in going from λ_i to λ_f, which gives

$$\Delta P_{n,\mathrm{i}\to\mathrm{f}} = \frac{-e}{2\pi} \iint_S \Omega_n^{(\lambda k)} \, d\lambda \, dk \tag{4.35}$$

where S is the rectangular region shown in Fig. 4.3. But Stokes' theorem, Eq. (3.30), tells us that the area integral of a Berry curvature is equal to the Berry phase evaluated around the boundary in the positive sense of circulation, so that

$$\Delta P_{n,\mathrm{i}\to\mathrm{f}} = \frac{-e}{2\pi} (\phi_A + \phi_B - \phi_C - \phi_D) \tag{4.36}$$

where ϕ_A and ϕ_C are integrals $\int_\mathrm{i}^\mathrm{f} A_n^{(\lambda)} \, d\lambda$ at two different values of k, while ϕ_B and ϕ_D are integrals $\int_0^{2\pi/a} A_n^{(k)} \, dk$ at two different values of λ, as illustrated in Fig. 4.3.

Recall that the Berry curvature $\Omega_n^{(\lambda k)}$ is gauge-invariant, so the expression Eq. (4.35) for ΔP is completely independent of the choice of gauge. Each of the four Berry phases on the right side of Eq. (4.36) is gauge-dependent, but Stokes' theorem tells us that if all four are defined for a gauge that is smooth and continuous everywhere in the interior of S and on its boundary, then Eq. (4.36) is true without any ambiguity modulo 2π.[5]

In Sec. 3.4 we said that we would normally insist on choosing a *periodic gauge* in k-space, and we shall do so now. As specified by Eq. (3.62), this means that for any given λ, such as the one indicated by the dotted vertical line in Fig. 4.3, $|\psi_{nk}\rangle$ is identical at the top and bottom of the BZ, as indicated by the two dots. We also insist that the gauge should be smooth as a function of λ. But if the states along segments A and C are identical, then we expect $\phi_A = \phi_C$, and two of the terms in Eq. (4.36) cancel! Since this is an important step, we check it via

$$\begin{aligned}
\phi_C &= i \int_\mathrm{i}^\mathrm{f} \langle u_{n,k=2\pi/a} | \partial_\lambda u_{n,k=2\pi/a} \rangle \, d\lambda \\
&= i \int_\mathrm{i}^\mathrm{f} \langle u_{n,k=0} e^{2\pi i x/a} | \partial_\lambda e^{-2\pi i x/a} u_{n,k=0} \rangle \, d\lambda \\
&= i \int_\mathrm{i}^\mathrm{f} \langle u_{n,k=0} | \partial_\lambda u_{n,k=0} \rangle = \phi_A
\end{aligned} \tag{4.37}$$

where Eq. (3.63) has been used in going from the first line to the second. Each of the remaining terms in Eq. (4.36) is just the kind of Berry phase defined in Eq. (3.61), i.e., the phase $\phi_n(\lambda)$ acquired as the Bloch state $|u_{nk}\rangle$

[5] If we only have a gauge that is smoothly defined on the boundary of S but not necessarily on its interior, then we would have to write $\Delta P_{n,\mathrm{i}\to\mathrm{f}} \coloneqq \frac{-e}{2\pi}(\phi_A + \phi_B - \phi_C - \phi_D)$ in the spirit of Eq. (1.6) or (3.36).

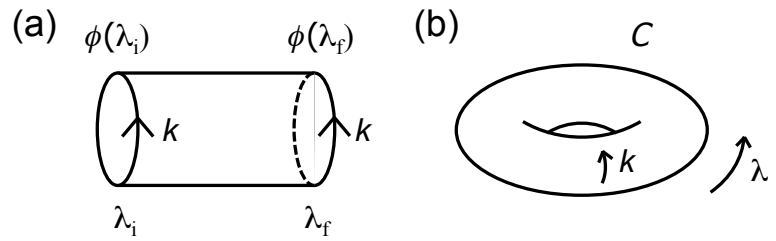

Figure 4.4 (a) Region S of Fig. 4.3, wrapped into a cylinder. Berry phases ϕ at boundary loops are indicated. (b) Same, but wrapped further into a torus in the case of a closed loop in λ space. Chern number C of the surface is indicated.

of band n is carried around the 1D BZ, evaluated either at $\lambda = \lambda_\mathrm{i}$ or λ_f. Restoring the sum over occupied bands, we then find the central result

$$\Delta P_{\mathrm{i}\to\mathrm{f}} = \frac{-e}{2\pi} \sum_n^{\mathrm{occ}} \left[\phi_n(\lambda_\mathrm{f}) - \phi_n(\lambda_\mathrm{i})\right] . \tag{4.38}$$

A useful way to think about the above derivation is to note that, having identified $k = 2\pi/a$ and $k = 0$ as being equivalent, we can think of the region S of Fig. 4.3 as being wrapped into a cylinder, as shown in Fig. 4.4(a). Then according to Stokes' theorem the integral of $\Omega_n^{(\lambda k)}$ on this cylinder is given by the Berry phase on the boundary, which in this case is composed of the two disconnected loops at the ends. After taking account of the sense of circulation on these loops, Stokes' theorem immediately yields Eq. (4.38).

With this equation, we have not only eliminated the undesirable sum over unoccupied states in Eq. (4.17), as was already accomplished in Eq. (4.31), but we have also expressed the change of polarization only in terms of calculations that can be carried out independently at the initial and final configurations λ_i and λ_f, with no detailed knowledge of the path connecting them. In fact, Eq. (4.38) can be recast simply as

$$\Delta P_{\mathrm{i}\to\mathrm{f}} = P(\lambda_\mathrm{f}) - P(\lambda_\mathrm{i}) \tag{4.39}$$

where the polarization of a 1D insulator is *defined* to be

$$P = \frac{-e}{2\pi} \sum_n^{\mathrm{occ}} \phi_n . \tag{4.40}$$

This formula is the central result of what is referred to as the "Berry phase theory" or "modern theory" of polarization.

Various alternative forms are possible. Equation (4.40) can be rewritten

in terms of the Berry potential $A_n(k) = i\langle u_{nk}|\partial_k u_{nk}\rangle$ as

$$P = \frac{-e}{2\pi} \sum_n^{\text{occ}} \int_0^{2\pi/a} A_n(k)\, dk\,. \tag{4.41}$$

As written these formulas only apply when each band n is isolated, but using the methods of Sec. 3.6.2 we can treat the entire group of occupied bands as a unit and write

$$P \;=\; \frac{-e}{2\pi}\,\phi \;=\; \frac{-e}{2\pi} \int_0^{2\pi/a} A^{\text{tr}}(k)\, dk \tag{4.42}$$

where ϕ is ϕ_{tot} of Eq. (3.107) and $A^{\text{tr}}(k)$ is given by Eq. (3.114). When the bands are isolated $\phi = \sum_n^{\text{occ}} \phi_n$ and $A^{\text{tr}}(k) = \sum_n^{\text{occ}} A_n(k)$, but the forms given in Eq. (4.42) are robust even in the presence of band degeneracies and crossings within the manifold of occupied states. When generalized to 3D (see Sec. 4.3), Eqs. (4.39) and (4.40) become

$$\Delta\mathbf{P}_{\text{i}\to\text{f}} = \mathbf{P}(\lambda_{\text{f}}) - \mathbf{P}(\lambda_{\text{i}}) \tag{4.43}$$

where

$$\mathbf{P} = \frac{-e}{(2\pi)^3} \sum_n^{\text{occ}} \int_{\text{BZ}} \mathbf{A}_n(\mathbf{k})\; d^3k \tag{4.44}$$

for isolated bands or

$$\mathbf{P} = \frac{-e}{(2\pi)^3} \int_{\text{BZ}} \mathbf{A}^{\text{tr}}(\mathbf{k})\; d^3k\,. \tag{4.45}$$

when treating the occupied bands as a unified group. All of these expressions are written assuming spinor bands; a factor of two should be inserted as usual whenever a spin-degenerate band convention is adopted.

4.2.3 Quantized diabatic charge transport in 1D

We shall have much to say in the next section about how to qualify and interpret the above Berry-phase experssions, especially as regards the 2π ambiguity in the Berry phases and the associated ambiguity in the polarization. For the moment we content ourselves with observing that, if the path is actually a closed path as in Fig. 1.5(b), so that λ_{i} and λ_{f} describe identical 1D Hamiltonians, then we can also "glue together" the two ends of the cylinder in Fig. 4.4(a) to get the torus shown in Fig. 4.4(b). Since the torus is a closed manifold, the Chern theorem of Eq. (3.37) applies to it, and one concludes that $\iint_S \Omega_n^{(\lambda k)}\, d\lambda\, dk$ must be 2π times an integer C, so that the adiabatically pumped charge described by $\Delta P_{\text{i}\to\text{f}}$ in Eq. (4.35) is

just e times an integer. This is precisely the quantization of adiabatic charge transport that was anticipated in Ch. 1.

4.2.4 Historical development

Before closing this section, it may be of interest to briefly recap the historical development of this theory. From the perspective of the computational electronic structure community, the first critical step was taken by Resta (1992), who focused attention on polarization differences as opposed to some absolute concept of polarization, and suggested that such differences could be calculated via Eq. (4.26) with $dP/d\lambda$ computed using Eq. (4.17) or (4.18). The remainder of the above derivation then appeared in a condensed but essentially similar form in King-Smith and Vanderbilt (1993). However, there were many important antecedents, stretching back to the foundational work of Blount (1962), who developed methods very early on for how to incorporate the position operator into the formalism of the Bloch representation. The most important precedent was almost certainly the paper of Thouless (1983), who first derived formulas for the adiabatically induced current and its time integral and understood their topological implications. Thouless essentially carried out the above derivation, although in a somewhat different language (notably, electric polarization was not mentioned) and with a focus on the quantization of charge transport for closed loops. This was around the same time as some of the foundational papers of Michael Berry, e.g., Berry (1984), and the work of Zak (1989) focusing on the concept of Berry phases of energy bands was another important precedent. Nevertheless, it was not until after the papers of Resta (1992) and King-Smith and Vanderbilt (1993) (which drew heavily on the 1983 Thouless paper) that the importance of these developments came to be understood in the computational electronic structure community.

Exercise 4.2.1

(a) Show that $\mathbf{v_k} = (\mathbf{p} + \hbar\mathbf{k})/m$ for a Hamiltonian of the form $H = p^2/2m + V(\mathbf{r})$.

(b) Show that $\langle u_{m\mathbf{k}}|\mathbf{v_k}|u_{m\mathbf{k}}\rangle = \langle u_{m\mathbf{k}}|\mathbf{p}|u_{m\mathbf{k}}\rangle/m$ for different bands $m \neq n$.

Exercise 4.2.2 Show that...

Exercise 4.2.3

4.3 Discussion

The arguments of the previous section imply that the polarization $\mathbf{P}$ cannot be expressed as the expectation value of a quantum operator, as is the case

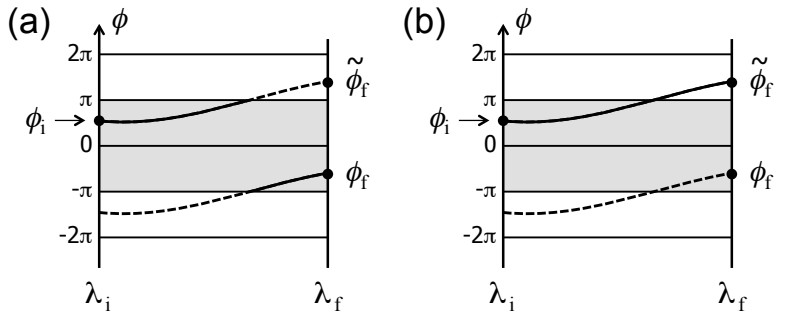

Figure 4.5 (a) Berry phase is assigned to branch choice $\phi \in [-\pi, \pi]$ (shaded region) independent of λ. (b) Branch choice is chosen in such a way that ϕ varies smoothly with λ. Solid and dashed curves differ by the quantum of 2π.

for most observable properties of quantum systems. Instead, it is related to Berry phases and Berry curvatures of the Bloch wavefunctions in reciprocal space. Since this situation is unfamiliar to most of us, it is worth discussing several aspects of the theory and clarifying some of its subtleties.

4.3.1 The quantum of polarization

Let us briefly review the discussion of the "quantum of polarization" that appeared earlier in Sec. 1.1.2, returning to the case of a 1D insulator. The left-hand side of Eq. (4.39) represents the time-integrated current that flows for a *particular* adiabatic path connecting the initial and final states, such as the one shown by a solid line in Fig. 1.5(a). It may be different for a different path such as the dashed-line one in Fig. 1.5(a), but if so it can only differ by the quantum, i.e., by an integer multiple of e.

The right-hand side of Eq. (4.39) can be interpreted in two different ways, depending on the context. If we have information only on the initial and final states, and not on the path connecting them, then each Berry phase ϕ_n should be regarded as defined only modulo 2π, so that $P(\lambda_i)$ and $P(\lambda_f)$ are each known only modulo e. In this case it is safer to rewrite Eq. (4.39) with the '=' sign replaced by the ':=' notation introduced in Ch. 1, e.g., in Eqs. (1.6) and (1.15); this indicates that the definite quantity on the left-hand side is equal to the right-hand side up to a quantum (here e). This is illustrated in Fig. 4.5(a), where $\phi = \sum_n^{\text{occ}} \phi_n$ is plotted versus λ. If we have no knowledge of the path, then we make some arbitrary branch choice, such as $\phi \in [0, 2\pi]$ as shown by the shaded region, and can conclude only that $\Delta P_{i\to f} = -e[(\phi_f - \phi_i)/2\pi + N]$ for some unknown integer N.

On the other hand, if we have full information about the path, and compute the Berry phase $\phi(\lambda)$ for each point along the path, then Eq. (4.39) becomes a true equality assuming that we insist that $\phi(\lambda)$ vary smoothly along the path as in Fig. 4.5(b), avoiding any 2π discontinuities like the one visible in Fig. 4.5(a). In this case we can conclude that $\Delta P_{\mathrm{i}\to\mathrm{f}} = -e(\widetilde{\phi}_{\mathrm{f}}-\phi_{\mathrm{i}})/2\pi$ with no uncertainty modulo the quantum.

Most commonly we will be working in the former context, where we are interested in P for some particular configuration; in this case we suppress the λ-dependence and just write P as in Eq. (4.40) or (4.41). There are several equivalent ways of thinking about the fact that P is only well-defined modulo the quantum e. One is to assign it some specific value on the real axis – say, $0.2\,e$ – but understanding that either $-0.8\,e$ or $1.2\,e$ would be an equivalent specification. A second is to wrap the real axis onto a circle of circumference e, and specify the value of P as a point on this circle. A third is to think of P as a *lattice-valued* quantity; that is, P is associated with the lattice of values $\{...,-1.8\,e,-0.8\,e,0.2\,e,1.2\,e,...\}$.

Quantities of this kind, that are only defined modulo a quantum, do not arise very frequently, but they are not entirely without precedent. To give one example, suppose you are standing in front of two mechanical clocks, each of which ticks once a second, one softly and one loudly, and you want to describe the relative phase of the ticks. Let's call this the asynchronicity A, defined as the time delay from a soft tick to a loud one. Specifying $A=0.2\,\mathrm{s}$ or $A=1.2\,\mathrm{s}$ or even $A=-0.8\,\mathrm{s}$ are obviously equivalent, and using the lattice-valued approach one could also say $A=\{...,-0.8\,\mathrm{s},0.2\,\mathrm{s},1.2\,\mathrm{s},...\}$. The polarization and the asynchronicity are two examples of physical quantities that are naturally defined only up to a quantum.

The generalization of the polarization formula from 1D to 3D is fairly obvious with reference to Eqs. (4.41) and (4.44), but it is usually better to avoid working with gauge-dependent quantities such $\mathbf{A}$, and the "modulo a quantum" nature of $\mathbf{P}$ is not obvious in this form. To clarify this aspect, let's return to Eq. (4.31) and make use of the relations between the primitive lattice vectors $\mathbf{a}_j$ and their reciprocal-space counterparts $\mathbf{b}_j$ ($j=\{1,2,3\}$). Note that for a function $f(\mathbf{k})$ defined on the BZ we can write

$$\frac{\partial f}{\partial \kappa_j} = \frac{\partial f}{\partial \mathbf{k}}\cdot\frac{\partial \mathbf{k}}{\partial \kappa_j} = \frac{\mathbf{b}_j}{2\pi}\cdot\partial_{\mathbf{k}} f$$

where the reduced wavevector components κ_j, each of which runs from 0 to 2π, were introduced in Eq. (2.30). Taking the inner product of $\mathbf{b}_j$ with both

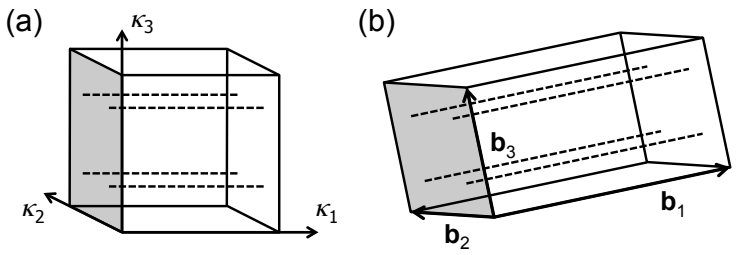

Figure 4.6 (a) Strings of k-points along which Berry phases are computed to obtain $\bar{\phi}_{n1}$, shown in the reduced BZ of variables $(\kappa_1, \kappa_2, \kappa_3)$ each of which runs between 0 and 2π. (b) Same, but shown in the parallelogram unit cell in the usual reciprocal space (k_x, k_y, k_z), illustrated for the case of a crystal of low symmetry.

sides of Eq. (4.31) then gives, for the contribution from occupied band n,

$$\begin{aligned} \mathbf{b}_j \cdot \partial_\lambda \mathbf{P}_n &= \frac{e}{(2\pi)^2} \int_{\mathrm{BZ}} 2\mathrm{Im}\, \langle \partial_\lambda u_{n\mathbf{k}} | \partial_{\kappa_j} u_{n\mathbf{k}} \rangle \, d^3k \\ &= \frac{-e}{(2\pi)^2} \int_{\mathrm{BZ}} \Omega_{\lambda j} \, d^3k \end{aligned} \tag{4.46}$$

where $\Omega_{\lambda j}$ is the Berry curvature of $|u_n(\lambda, \kappa_1, \kappa_2, \kappa_3)\rangle$ with respect to variables λ and κ_j. The volume elements are related by $d^3\kappa = V_{\mathrm{cell}}\, d^3k$; converting to an integral over κ space, specializing temporarily to $j = 1$, and making a similar argument to the one leading to Eq. (4.38) in 1D, we find

$$\mathbf{b}_1 \cdot \mathbf{P}_n = \frac{-e}{V_{\mathrm{cell}}} \frac{1}{(2\pi)^2} \iint \phi_{n1}(\kappa_2, \kappa_3) \, d\kappa_2 \, d\kappa_3 \tag{4.47}$$

where the κ_2 and κ_3 integrals run over $[0, 2\pi]$ and

$$\phi_{n1}(\kappa_2, \kappa_3) = \int_0^{2\pi} i \langle u_{n\boldsymbol{\kappa}} | \partial_{\kappa_1} u_{n\boldsymbol{\kappa}} \rangle \, d\kappa_1 \tag{4.48}$$

is the Berry phase of band n computing along a string of $\mathbf{k}$-vectors in the BZ extending parallel to $\mathbf{b}_1$.

The situation is illustrated in Fig. 4.6. The k-point strings along which the Berry phases ϕ_{n1} need to be computed are shown in panel (a) in the $\boldsymbol{\kappa}$-space BZ, which is a cube of side 2π. These Berry phases could equivalently be computed along the strings parallel to reciprocal lattice vector $\mathbf{b}_1$ in the true $\mathbf{k}$-space parallelogram BZ in panel (b). Note that Eq. (4.47) instructs us to average $\phi_{n1}(\kappa_2, \kappa_3)$ over the (κ_2, κ_3) plane; call this average $\bar{\phi}_{n1}$. Also let $\bar{\phi}_{n2}$ be the average of $\phi_{n2}(\kappa_1, \kappa_3)$ over the (κ_1, κ_3) plane, where the Berry phases are now taken for strings along κ_2 (or parallel to $\mathbf{b}_2$), and similarly

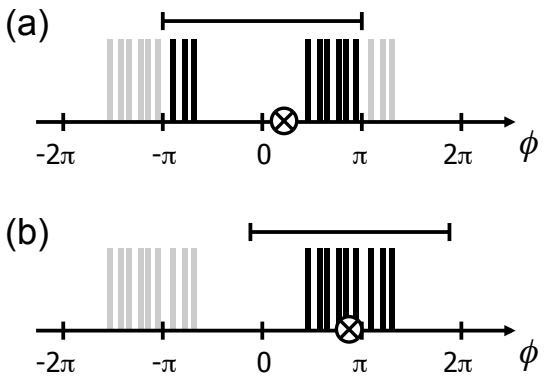

Figure 4.7 Histograms of Berry phases computed for parallel k-point strings on a sampling of the orthogonal face of the 2D BZ (see Fig. 4.6).

for $\bar{\phi}_{n3}$. Then Eq. (4.47) becomes just or

$$\mathbf{b}_j \cdot \mathbf{P}_n = \frac{-e}{V_{\text{cell}}} \bar{\phi}_{nj} \,. \tag{4.49}$$

Restoring the sum over bands, this becomes

$$\mathbf{P} = \frac{-e}{V_{\text{cell}}} \sum_j \frac{\bar{\phi}_j}{2\pi} \mathbf{a}_j \tag{4.50}$$

where $\bar{\phi}_j = \sum_n^{\text{occ}} \bar{\phi}_{nj}$, as is easily checked by multiplying by $\mathbf{b}_{j'}$. When treating all occupied bands as a unified group, one replaces the individual $\phi_{n1}(\kappa_2, \kappa_3)$ of Eq. (4.48) by a total $\phi_1(\kappa_2, \kappa_3)$ defined in the manner of Eq. (3.107); then $\bar{\phi}_1$ is defined as its average over the (κ_2, κ_3) plane, and similarly for $\bar{\phi}_2$ and $\bar{\phi}_3$.

The quantum of indeterminacy in the definition of $\mathbf{P}$ is now clearly evident in Eq. (4.50). Each Berry phase is insensitive to a change $\bar{\phi}_j \to \bar{\phi}_j + 2\pi m_j$, which amounts to shifting $\mathbf{P}$ by $(-e/V_{\text{cell}})\mathbf{R}$ where $\mathbf{R}$ is the real-space lattice vector $m_1\mathbf{a}_1 + m_2\mathbf{a}_2 + m_3\mathbf{a}_3$. This is exactly the indeterminacy that was anticipated in Eq. (1.7).

There is a subtlety in the definition of the average Berry phase $\bar{\phi}_j$ that should not be overlooked. For $\bar{\phi}_1$ to make sense, we need to insure that $\phi_1(\kappa_2, \kappa_3)$ is a smooth function of κ_2 and κ_3 with no 2π jumps. The difficulty is illustrated in Fig. 4.7, where we imagine that the 2D (κ_2, κ_3) face of the BZ has been sampled with a 3×3 sampling mesh, and the nine resulting Berry phases are shown as a histogram. It would be a mistake to make the branch choice $\phi \in [-\pi, \pi]$ for each phase individually as in Fig. 4.7(a); the resulting average $\bar{\phi}$, shown as the circled cross, would be meaningless. If the

branch choice is made arbitrarily for one k-point string and then the others are chosen such that $|\Delta\phi| << 2\pi$, then a clustered group of Berry phases is correctly identified as in Fig. 4.7(b), and the average $\bar{\phi}$ is suitable for use in Eq. (4.50).

It is important to note that the indeterminacy of $\mathbf{P}$ modulo a quantum is rarely a problem in practice. In virtually all dielectrics, the change $\Delta\mathbf{P}_{\mathrm{i}\to\mathrm{f}}$ that can be induced by applying a moderate electric field (e.g., whose strength is insufficient to cause dielectric breakdown) is a small fraction of the quantum $e\mathbf{R}/V_{\mathrm{cell}}$, and the same is true for most ferroelectrics upon reversal of the spontaneous polarization by an external field. In this case the appropriate algorithm is to make an arbitrary branch choice when computing the three $\bar{\phi}_j(\lambda_{\mathrm{i}})$, and then choose the branch for each computed $\bar{\phi}_j(\lambda_{\mathrm{f}})$ such that $|\bar{\phi}_j(\lambda_{\mathrm{f}}) - \bar{\phi}_j(\lambda_{\mathrm{i}})| << \pi$. In some unusual cases, as for strongly polarized ferroelectrics such as $PbTiO_3$ or $BiFeO_3$, it may be that the difference can approach or exceed π; in this case the best practical solution is to compute $\mathbf{P}$ on a few intermediate values of λ between λ_{i} and λ_{f}, making sure that the branch choices are consistent for each neighboring pair of λ values.

4.3.2 Ionic contribution and origin dependence

Strictly speaking, the polarization $\mathbf{P}$ given by Eq. (4.44) or (4.50) is only the electronic contribution. If the atoms are moving during the adiabatic evolution parametrized by λ, then the currents associated with the classical motions of the charged nuclei also have to be taken into account. We can easily adapt the formalism developed in Sec. 1.1.4 to express this "ionic" contribution

$$\mathbf{P}_{\mathrm{ion}} = \frac{1}{V_{\mathrm{cell}}} \sum_s e Z_s \boldsymbol{\tau}_s \,. \tag{4.51}$$

Here $\boldsymbol{\tau}_s$ gives the location of the nucleus s in the unit cell, while Z_s specifies either the atomic number in the case of all-electron calculations, or the core charge in the case of pseudopotential calculations. As discussed in Sec. 1.1.4, an expression of the form of Eq. (4.51) is also well-defined only modulo the quantum $e\mathbf{R}/V_{\mathrm{cell}}$, since each $\boldsymbol{\tau}_s$ is arbitrary modulo $\mathbf{R}$. Combining Eqs. (4.50) and (4.51) gives

$$\mathbf{P}_{\mathrm{tot}} = \frac{e}{V_{\mathrm{cell}}} \left[\sum_s Z_s \boldsymbol{\tau}_s - \sum_j \frac{\bar{\phi}_j}{2\pi} \mathbf{a}_j \right] . \tag{4.52}$$

The quantity in brackets is well-defined modulo a lattice vector $\mathbf{R}$, so that $\mathbf{P}_{\mathrm{tot}}$ is well-defined modulo $e\mathbf{R}/V_{\mathrm{cell}}$.

If Eq. (4.52) is a valid expression for the polarization, it should be invariant against a translation of the contents of the unit cell by some common vector $\mathbf{t}$, or equivalently, a translation of the origin by $-\mathbf{t}$. The change of $\mathbf{P}_{\rm ion}$ under such a shift is $\Delta\mathbf{P}_{\rm ion} = (Q^+_{\rm cell}/V_{\rm cell})\mathbf{t}$, where $Q^+_{\rm cell} = e\sum_s Z_s$ is the total nuclear or ionic charge in the unit cell, so this term by itself is clearly not invariant. To understand what happens to the electronic contribution, it is easiest to return to Eq. (4.44). After the translation, the new Bloch functions are related to the old ones by $\tilde{\psi}_{n\mathbf{k}}(\mathbf{r}) = \psi_{n\mathbf{k}}(\mathbf{r}-\mathbf{t})$ from which it follows that $\tilde{u}_{n\mathbf{k}}(\mathbf{r}) = e^{-i\mathbf{k}\cdot\mathbf{t}}\,u_{n\mathbf{k}}(\mathbf{r})$ and thus $\tilde{\mathbf{A}}_{n\mathbf{k}} = \mathbf{A}_{n\mathbf{k}} + \mathbf{t}$. The change in the electronic contribution of Eq. (4.44), which we temporarily denote as $\mathbf{P}_{\rm elec}$, is therefore $\Delta\mathbf{P}_{\rm elec} = -eN_{\rm occ}\mathbf{t}V_{\rm BZ}/(2\pi)^3$. Using $V_{\rm BZ} = (2\pi)^3/V_{\rm cell}$ and letting $Q^-_{\rm cell} = -eN_{\rm occ}$ be the total electronic charge in the unit cell, this becomes $\Delta\mathbf{P}_{\rm elec} = (Q^-_{\rm cell}/V_{\rm cell})\mathbf{t}$. Finally, overall cell neutrality implies that $Q^-_{\rm cell} = -Q^+_{\rm cell}$, so that $\mathbf{P}_{\rm tot} = \mathbf{P}_{\rm ion} + \mathbf{P}_{\rm elec}$ is indeed invariant under global translations of the crystal.

4.3.3 Relation to Wannier charge centers

Recall that in Sec. 3.5.1 we derived Eq. (3.83) expressing the center of charge of a Wannier function constructed for band n as

$$\bar{\mathbf{r}}_n = \frac{V_{\rm cell}}{(2\pi)^3}\int_{\rm BZ}\mathbf{A}_n(\mathbf{k})\,d^3k\,. \tag{4.53}$$

The astute reader may have noticed the remarkable similarity of this equation to Eq. (4.44), our Berry-phase formula for $\mathbf{P}$. In fact, combining these two equations, one finds that

$$\mathbf{P} = \frac{-e}{V_{\rm cell}}\sum_n^{\rm occ}\bar{\mathbf{r}}_n\,, \tag{4.54}$$

so that the electronic contribution to polarization is determined entirely by the Wannier centers of the occupied bands! In fact, the total polarization of Eq. (4.52) can be written as

$$\mathbf{P}_{\rm tot} = \frac{e}{V_{\rm cell}}\left[\sum_s Z_s\,\boldsymbol{\tau}_s - \sum_n \bar{\mathbf{r}}_n\right]. \tag{4.55}$$

The expressions given above assume that all bands n are isolated. For the multiband case discussed in Sec. 3.6.1, one constructs J Wannier functions $|w_{n\mathbf{R}}\rangle$ that exactly span the J occupied bands of the insulating crystal, although these Wannier functions no longer have a one-to-one correspondence

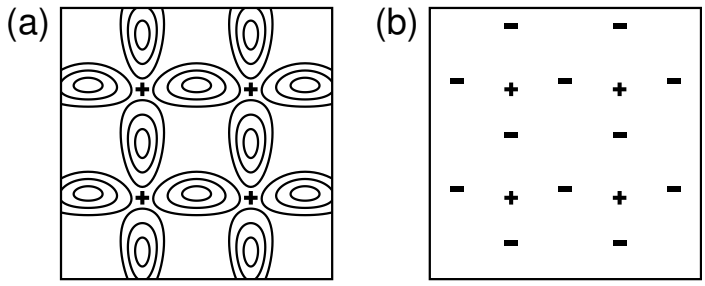

Figure 4.8 Mapping of the true crystalline charge density of an insulator, sketched in (a), onto a point-charge model, as in (b). Contours indicate electronic charge clouds of the real system; '+' symbols denote nuclei carrying charge $+2e$; and '−' symbols indicate integer charges $-e$ located at the Wannier center positions.

with the Bloch eigenstates $|\psi_{n\mathbf{k}}\rangle$, having been constructed as linear combinations of different bands.[6] Nevertheless, Eq. (4.53) can be replaced by

$$\sum_n \bar{\mathbf{r}}_n = \frac{V_{\text{cell}}}{(2\pi)^3} \int_{\text{BZ}} \mathbf{A}^{\text{tr}}(\mathbf{k})\, d^3k \tag{4.56}$$

as will be shown in Ex. 4.3.2, and comparing with Eq. (4.45) it follows that Eq. (4.54) still holds.

Equation (4.55) has a remarkably simple interpretation. Recall that in Sec. 1.1.4 we considered a fictitious physics in which both the positive and negative charges making up a crystal come packaged as point charges carrying an integer multiple of the charge quantum e. For such a system, we argued that we could define the polarization via Eq. (1.18), namely $\mathbf{P} = (e/V_{\text{cell}}) \sum_j Z_j \boldsymbol{\tau}_j$, where j runs over the charges eZ_j located at $\boldsymbol{\tau}_j$ in the unit cell. Since each $\boldsymbol{\tau}_j$ is only well-defined modulo a lattice vector, this definition of $\mathbf{P}$ is only well-defined modulo $\mathbf{P}$, as it should be. But Eq. (4.55) takes exactly this form, with the nuclei (or pseudo ions) appearing as positive charges $Z_j > 0$, and the electrons appearing as point charges with $Z_j = -1$ located at the Wannier centers.

This provides an insightful way to think about the Berry-phase theory of polarization. The true physical charge distribution in an insulating crystal is sketched in Fig. 4.8(a); the nuclei can be treated as integer point charges,[7] but the electrons form smeared-out charge distributions whose probability

[6] That is, the index n in $\bar{\mathbf{r}}_n$ does *not* have the same meaning as in $|\psi\rangle_{n\mathbf{k}}$, although both run from 1 to J.

[7] Nuclei have dimensions of femtometers, which is negligible on the atomic scale. In the context of pseudopotential calculations, the nuclear charges are replaced by core charges whose size can be on the order a bohr. However, these are strictly localized and non-overlapping

distribution is given by the Schrödinger equation. It is this latter fact causes all the trouble, but now we see a way out! We set up a mapping from the true quantum system to one in which the nuclei continue to appear as point charges, but the distributed electron charge clouds are replaced by $-e$ point charges located at the Wannier centers. We then define the polarization of our true system to be that of the mapped system as given by Eq. (1.18). Equation (4.55) tells us that this definition is entirely equivalent to the Berry-phase formulas like Eq. (4.44) or (4.50) given above. This interpretation will be especially useful in the discussion of the surface charge theorem in Sec. 4.5.

4.3.4 Practicalities

Here we give a few comments that will be of most interest to users of first-principles DFT electronic structure codes developed for the study of crystalline solids. By now almost all such codes have a capability for computing the Berry-phase polarization. We first review how the calculation is typically implemented in practice, and then discuss some considerations that should be kept in mind in the process of doing the calculations.

Typically most of the computer time in DFT and related methods, as introduced on p. 35, is devoted to the self-consistent field (SCF) iteration to the ground state for a given set of nuclear coordinates, which is often repeated in an outer iterative loop to allow for structural relaxation. The polarization typically needs to be computed only at the end of this process, and is usually much less expensive because a one-shot calculation using the previously converged Kohn-Sham potential can be used. In this sense, it is similar to the calculation of bandstructures and densities of states. In particular, the k-point sampling need not be the same as the one used in the SCF calculation.

The calculation basically proceeds in the manner of Eq. (4.50) as illustrated in Fig. 4.6. The user chooses a primitive real-space lattice vector $\mathbf{a}_j$ as the direction for which the component of $\mathbf{P}$ (i.e., the average phase $\bar{\phi}_j$) is going to be calculated. In some cases the choice of $\mathbf{a}_j$ is obvious from the start, as for a tetragonal or rhobohedral ferroelectric where symmetry constrains the polarization to lie along the symmetry axis, or for a superlattice calculation where one is only interested in the polarization normal to the layers. In a more general case, one just starts with the first primitive vector

spherical charge distributions, so that by Gauss' law they too can be treated as though they were true point charges.

$\mathbf{a}_1$ and then repeats the entire procedure independently for $\mathbf{a}_2$ and $\mathbf{a}_3$, and later assembles the full polarization using Eq. (4.50).

For a given $\mathbf{a}_j$, then, the user is asked to choose a mesh sampling scheme in k-space. Typically this is a regular mesh in the two k-space directions orthogonal to $\mathbf{a}_j$, with a density similar to that used for the SCF part of the calculation (shown as 2×2 in Fig. 4.6, but typically somewhat denser). Then, to insure good convergence for the k-point extending along the $\mathbf{b}_j$ direction, shown as dashed lines in Fig. 4.6, one usually requests a finer grid, perhaps with 10 or even 20 equally spaced k-points along the path. Empirically it is found that the convergence of the Berry phase with respect to the density of the 1D k-point mesh is slower than that of conventional observables that are sampled in the manner of Eq. (2.41), so some testing of the convergence of the results with respect to this mesh density is recommended.[8]

The code then computes a Berry phase along each k-point string, using the multiband formulation of Sec. 3.6.2 to treat the set of all occupied bands as a group. For each neighboring pair of points $\mathbf{k}_i$ and $\mathbf{k}_{i+1}$ along the string, the code computes the inner product matrix $M_{mn}^{(i,i+1)} = \langle u_{m\mathbf{k}_i} | u_{n\mathbf{k}_{i+1}} \rangle$ for each $i = \{0, ..., N-1\}$. This step is rather trivial in a plane-wave basis, but requires more care in the context of ultrasoft pseudopotential, augmented-wave, muffin-tin-orbital, or localized-orbital approaches. Note that $M_{mn}^{N-1,N}$ is computed as $\langle u_{m\mathbf{k}_{N-1}} | e^{-i\mathbf{b}_j \cdot \mathbf{r}} | u_{n\mathbf{k}_0} \rangle$ to account for the fact that the string winds around the BZ as in Eq. (3.64).

The Berry phase is usually then just computed from Eq. (3.110), i.e., from the product of the M matrices[9]

$$\phi = -\mathrm{Im} \ln \det \prod_{i=0}^{N-1} M^{(i,i+1)} \tag{4.57}$$

or an equivalent formula such as $-\mathrm{Im} \ln \prod \det M$ or $-\mathrm{Im} \sum \ln \det M$. Note that this formula has the nice feature of being exactly gauge-invariant, i.e., insensitive to any unitary rotation among the occupied states at a given k-point, as shown in Ex. 4.3.1. Thus, there is no need to construct a smooth gauge in advance of this calculation; any set of occupied Bloch states on the mesh, even if they are chosen with random individual phases, and random unitary rotations among degenerate states, yields exactly the same result.

[8] The convergence is typically exponential in the case of conventional observables, but only power-law for the Berry phase. Algorithms have been proposed to improve the convergence; see, e.g., Stengel and Spaldin (2006).

[9] As discussed in Sec. 3.6.2, one can alternatively evaluate the expression in Eq. (3.109), in which the M matrices have been replaced by their unitary approximants $\mathcal{M}$ using the procedure of Eqs. (3.103) and (3.104). This procedure is somewhat closer to the spirit of parallel transport, but involves additional operations. Both formulas tend to the same continuum limit as the mesh density gets fine.

As a reminder, in 3D one computes $\phi_1(\kappa_2, \kappa_3)$ on a 2D mesh in (κ_2, κ_3) as illustrated in Fig. 4.6, and then takes the average to get $\bar{\phi}_1$ (and similarly for $\bar{\phi}_2$ and $\bar{\phi}_3$). In doing this average, the individual values have to be clustered such that the branch choice treats all of them as a group, as illustrated in Fig. 4.7. Most code packages have implemented an algorithm for doing this grouping automatically. Similar considerations apply in 2D.

Incidentally, if one has access to a set of Wannier charge centers $\bar{\mathbf{r}}_n$ for all the occupied states, as for example if one is using WANNIER90 to compute maximally-localized Wannier functions for some other purpose, then another option is to compute $\mathbf{P}$ from the Wannier-center expression, Eq. (4.54). The result is usually not quite as well converged with respect to k-point sampling, however, unless a relatively dense k mesh is used in all three dimensions.

In practical calculations, the user should always be on the lookout for artifacts associated with the quantum of polarization. Each code typically uses some algorithm to make a branch choice for each $\bar{\phi}_j$, typically $-\pi < \bar{\phi}_j \leq \pi$, but it may or may not apply a similar reduction to the first term of Eq. (4.52), and if so, either before or after combining with the electronic term. Thus, it could be that different code packages might report different $\mathbf{P}$ values (different only modulo $e\mathbf{R}/V_{\text{cell}}$) using the same physical approximations for the same crystal. Also, when carrying out a series of calculations in which some structural parameter is modified, or as a function of strain or some other external field, the calculated $\mathbf{P}$ might "jump by a quantum." An additional source of potential confusion is that when running spin-degenerate calculations, an extra factor of two is inserted into the second term of Eq. (4.52) to reflect the spin degeneracy. If at least one of the constituents of the crystal is from an odd-numbered column of the Periodic Table, the ionic term in Eq. (4.52) is only well-defined modulo $e\mathbf{R}/V_{\text{cell}}$, while the electronic one is modul $2e\mathbf{R}/V_{\text{cell}}$. If all atoms are from even columns, than a quantum of $2e\mathbf{R}/V_{\text{cell}}$ can be used consistently for all terms.

Luckily, the changes in polarization that one is interested in are usually small compared to the quantum. Suppose, for example, that you have done a series of calculations for some ferromagnetic Ti compound in which both the tetragonal axis and the polarization are along $\hat{z}$, and you have displaced the Ti sublattice along z in increments of 0.2 Å from one calculation to the next. If you find values of 0.39, 0.43, 0.47, −0.45, and $-0.39\,\mu\text{C/cm}^2$ respectively, you should immediately suspect that there has been a jump by a quantum. Calculating the quantum as ec/a^2, where a and c are the in-plane and out-of-plane lattice constants respectively, suppose you find this to be $0.97\,\mu\text{C/cm}^2$. Then you should adjust the last two values by hand to

be 0.52 and 0.58 μC/cm^2 respectively, and the polarization difference ΔP_z from the first to the last configuration should be reported as 0.19 μC/cm^2.

In case some doubt remains about the correct branch choice for $\Delta\mathbf{P}$, as when the structural change is substantial and computed $\mathbf{P}$ values for intermediate configurations are not available, another useful heuristic is to estimate $\Delta\mathbf{P}$ using a rough model based on nominal ionic charges, treating the crystal as composed of rigid ions carrying these charges. That is, we estimate the change of polarization as

$$\Delta\mathbf{P}_{\text{nom}} = \frac{e}{V_{\text{cell}}} \sum_s Z_{\text{nom},s}\, \Delta\boldsymbol{\tau}_s \,, \tag{4.58}$$

where the nominal charge $Z_{\text{nom},s}$ is identified with the formal ionic charge of atom s. If we are considering a structural change in Fe_2O_3, for example, we treat Fe as trivalent and assign charges $Z_{\text{nom}}(\text{Fe}) = +3$ and $Z_{\text{nom}}(\text{O}) = -2$. Since we presumably know the path taken by the ions during the structural change, there is no ambiguity about the atomic displacements $\Delta\boldsymbol{\tau}_s$, and thus, no uncertainty about the branch choice of $\Delta\mathbf{P}_{\text{nom}}$. This estimate may be quite rough, but this shouldn't matter, as it is only used as a guide for making the correct branch choice. That is, $\Delta\mathbf{P}$ is actually computed from the Berry-phase theory, and then the uncertainty modulo $e\mathbf{R}/V_{\text{cell}}$ is resolved by choosing the value closest to $\Delta\mathbf{P}_{\text{nom}}$.[10]

Let me close this subsection with a brief discussion of a philosophical question that arises in the context of the formal density-functional theory introduced in Sec. 2.1.1. We know that in principle the exact Kohn-Sham version of DFT (i.e., using the exact but unknown XC functional) should give the exact ground-state charge density and total energy, but is *not* exact for the ground-state wavefunction, band gap, and many other observables. Into which category does the Berry-phase polarization fall? The polarization is closely related to the charge density, and for a finite system the electric dipole clearly does have the sanction of the exact Kohn-Sham theory. But we have emphasized that the Berry-phase polarization depends instead on *currents* that flow during an adiabatic evolution, and these do not have the exact Kohn-Sham sanction. In fact the question is quite subtle; it seems the answer depends on boundary conditions in a rather nonlocal manner. The interested reader is referred to Vanderbilt (1997) for further discussion. In practice, experience has shown that polarization differences can be computed

[10] If the appropriate branch choice is still not clear using the nominal ionic charge model, an improved estimate can usually be obtained by using the Born effective charges, defined in Eq. (4.19) as the first-order change in $\mathbf{P}$ resulting from a change in the coordinates $\boldsymbol{\tau}_s$ of sublattice s. The Born-charge values can either be taken from the literature or computed in a relevant reference configuration.

using standard LDA or GGA versions of DFT with an accuracy comparable to that of other quantities of interest, such as energy differences, elastic constants, or phonon frequencies. Moreover, the experimental uncertainties in the measurement of $\mathbf{P}$ are often larger than for these other quantities, so this issue does not appear to be a pressing one in practice.

Exercise 4.3.1 Demonstrate the multiband gauge invariance claimed just below Eq. (4.57). In particular, suppose we rotate the states at $\mathbf{k}_{i'}$ to become $|\tilde{u}_{n\mathbf{k}_{i'}}\rangle = \sum_m U_{mn} |u_{m\mathbf{k}_{i'}}\rangle$. Show that the new ϕ computed from Eq. (4.57) using the new states is exactly the same as the old one.

Exercise 4.3.2

Here we demonstrate Eq. (4.56), assuming we already have a set of multiband Wannier functions in hand. (If you did not previously do Ex. 3.6.1, do it now, as it will be needed.)

(a) We first evaluate Eq. (4.56) using the particular gauge corresponding to the given set of Wannier functions via Eq. (3.94), whose reverse transform is

$$|\tilde{\psi}_{n\mathbf{k}}\rangle = \sum_{\mathbf{R}} e^{i\mathbf{k}\cdot\mathbf{R}} |w_{n\mathbf{R}}\rangle \,.$$

Show that this results in Eq. (4.56).

(b) Show that any other multiband gauge choice would give the same result modulo a lattice vector. Hint: Use the result of Ex. 3.6.1 and argue about the boundary conditions on $\beta(\mathbf{k})$.

Exercise 4.3.3

4.4 Questions of interpretation

As long as one is interested in computing the change in polarization from one reference configuration to another, the resolution of the quantum in the definition $\Delta\mathbf{P}$ can be carried out following the discussion above. However, in practice one would often like to discuss the polarization $\mathbf{P}$ for a given configuration. In this case, the issues of interpretation of the quantum can become even more confusing.

As an example, suppose we are interested in the spontaneous polarization P_s of $KNbO_3$ in its observed tetragonal structure at ?? K. Experimental literature values of P_s are around $40\,\mu C/cm^2$, but we would like to check this using a DFT calculation. The structure of an up-polarized domain of tetragonal $KNbO_3$ is shown in Fig. 4.9(a). It is a distorted version of a simple cubic perovskite structure in which the K, O, and Nb atoms lie at the face corners, face centers, and body centers, respectively; the ferroelectric

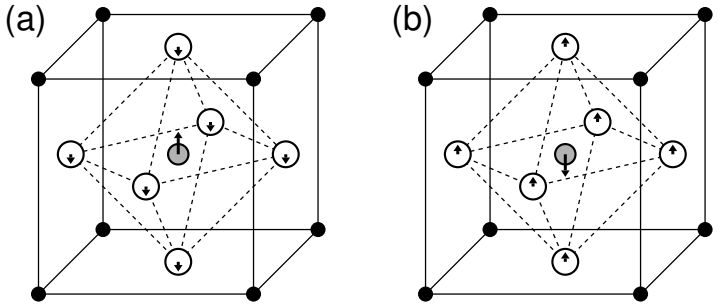

Figure 4.9 Text...

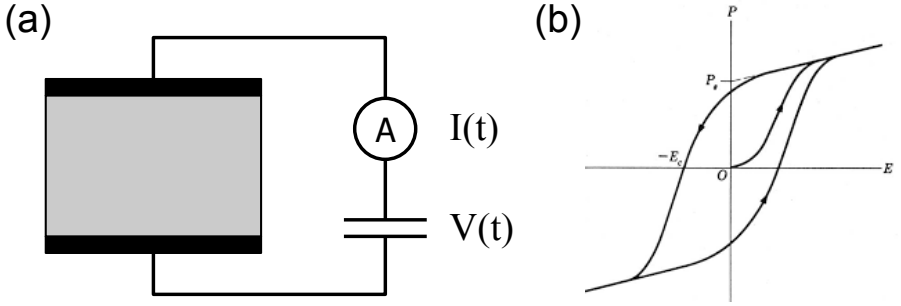

Figure 4.10 Text...

distortion corresponds to a displacement of the central Nb along $+\hat{z}$ relative to the surrounding oxygens. The opposite polarization state is illustrated in Fig. 4.9(b).

The DFT calculation proceeds by starting the Nb atom with some displacement, say 0.2 Å, along $+\hat{z}$, and relaxing the unit cell dimensions and internal coordinates subject to the tetragonal symmetry. When the structure has relaxed, we compute the Berry-phase polarization and find it reported as $86\,\mu\mathrm{C/cm}^2$. This is nowhere close to the observed value! The quantum $eR_{[001]}/V_{\mathrm{cell}} = e/a^2$ is reported as $102\,\mu\mathrm{C/cm}^2$, so adding or subtracting this from $86\,\mu\mathrm{C/cm}^2$ is clearly not going to help the agreement with experiment.

What went wrong?

4.4.1 How is polarization measured?

Let's first be sure we understand the meaning of the experimental value of the spontaneous polarization P_s. There is no way of measuring $\mathbf{P}_s$ directly; in practice it is always measured by observing the *switching current* that

flows during a reversal of the polarization by an external bias. That is, it is determined by hysteresis-loop measurements.

An example is shown in Fig. 4.10. The experimental setup is sketched in panel (a); a time-varying bias $V(t)$ is applied and the current $I(t)$ is measured flowing through the ammeter. The measured hysteresis curve is illustrated in panel (b); the vertical axis is really just a measure of the integrated current $Q(t) = \int I(t)\,dt$ that passed from one capacitor plate to the other. Starting from an unpoled sample (equal populations of up and down domains) at the origin of panel (b), a positive voltage is applied until the polarization P rises and saturates, at which point the entire sample is uniformly up-polarized. Reversing the bias carries the system along the top-left path; reversing it again results in the bottom-right path. E_C marks the coercive field, i.e., the value of the reversing electric field needed to transform half the sample into the opposite-domain state. The spontaneous polarization P_s is marked on the diagram; it is an extrapolated estimate of the polarization that a single uniform up domain would have at $E=0$.

In short, what is *actually measured* is the current that flows during the polarization reversal; since this is essentially $2P_s$, one divides by two (and by the area of the plates) to get the spontaneous polarization. So we are back to polarization as a difference. Theoretically, we should interpret P_s as being half of the ΔP in going from the structure of Fig. 4.9(b) to that of Fig. 4.9(a); or equivalently, the ΔP to go from a centrosymmetric cubic reference structure to the structure of Fig. 4.9(a).

So now suppose we carry out a DFT Berry-phase calculation of the polarization in the down-domain state of Fig. 4.9(b) and find that the code reports it as $16\,\mu\mathrm{C/cm^2}$. From one perspective this is good news: combining with our previous result of $86\,\mu\mathrm{C/cm^2}$ for the structure of Fig. 4.9(a), we get $P_s = (86-16)/2 = 35\,\mu\mathrm{C/cm^2}$, in very reasonable agreement with experiment.

But we may now be more confused then ever. Figures 4.9(a) and (b) are inversion images of one another, so the polarization ought to be reversed in going from one to the other. How can the computed values of 86 and $16\,\mu\mathrm{C/cm^2}$ make sense in this context?

As a last-ditch effort, we try setting the coordinates of our structure halfway between those in panels (a-b) of Fig. 4.9, i.e., in the centrosymmetric structure, thinking that by symmetry we must get $P=0$. Instead, the code reports $P=51\,\mu\mathrm{C/cm^2}$. Is something terribly wrong?

4.4.2 "Formal" vs. "effective" polarization

Let's see what we get if we treat centrosymmetric $KNbO_3$ using the nominal ionic model discussed on p. 139. In the spirit of Eq. (1.18) we are now applying this model to obtain the polarization itself via

$$\mathbf{P}_{\text{nom}} = \frac{e}{V_{\text{cell}}} \sum_s Z_{\text{nom},s}\, \boldsymbol{\tau}_s \,, \tag{4.59}$$

rather than just to a change in polarization as in Eq. (4.58). We adopt nominal ionic charges of 1, 5 and −2 for K, Nb, and O respectively, and set $\boldsymbol{\tau}_j$ to the ideal coordinates. Taking the origin on the K ion, we get $P_z = (1/a^2c)[(e)(0) + (5e)(c/2) + (-2e)(c/2 + c/2 + 0)] = e/2a^2$. This is half the quantum, or $102/2 = 51\,\mu\text{C/cm}^2$, exactly what we obtained from the DFT calculation above!

The resolution of all these apparently confusing results comes from remembering that the Berry-phase polarization is inherently a multivalued quantity, as emphasized on p. 130. Let's restate the results reported above in this language. For the up-domain state, the "value" of P_z is the lattice $\{..., -118, -16, 86, ...\}\,\mu\text{C/cm}^2$, while for the down-domain state it is $\{..., -86, 16, 118, ...\}\,\mu\text{C/cm}^2$. Sure enough, these "values" are interchanged by a sign reversal, as they must be under inversion.

When the crystal is centrosymmetric, the lattice of values must map to itself under inversion. If the quantum is $102\,\mu\text{C/cm}^2$ as assumed above, then there are only two possibilities for P_z consistent with inversion symmetry. One is $\{..., -102, 0, 102, ...\}\,\mu\text{C/cm}^2$, while the other is $\{..., -51, 51, ...\}$ $\mu\text{C/cm}^2$. Evidently centrosymmetric $KNbO_3$ belongs to the latter case, as does our classical calculation within the extreme ionic limit. These two calculations were destined either to agree perfectly, or else differ by exactly half a quantum. (As it happens, the former case applies.)

But this is a remarkable result. We are saying that the polarization of centrosymmetric $KNbO_3$ is not zero! More precisely, we are saying that the lattice-valued polarization of $KNbO_3$ does not contain zero as one of its values, but instead straddles zero in a symmetric fashion. The situation is shown graphically as projected onto the x-z plane in Fig. 4.11. Panels (a) and (b) show two possibilities for $\mathbf{P}$ that are both consistent with inversion symmetry; $KNbO_3$ belongs to case (b). When the crystal becomes spontaneously polarized along the $\hat{z}$ direction, the polarization lattice shifts upwards to the configuration shown in Fig. 4.11(c), and the change in polarization is indicated by the grey arrow at left in Fig. 4.11(c).

If you are a theorist, I do not recommend that you should run next door to your experimental colleage and try to explain that the polarization of

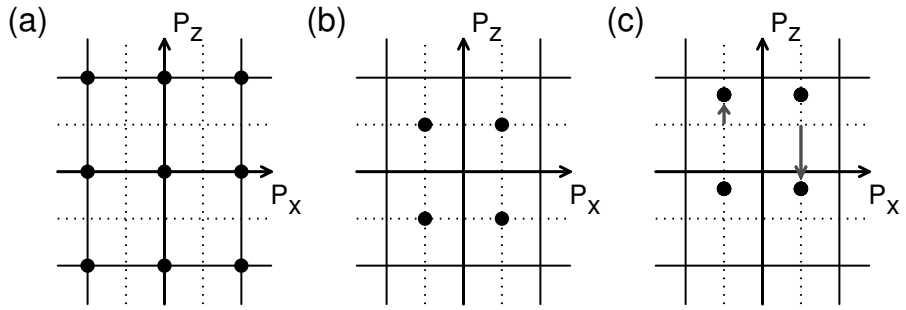

Figure 4.11 Polarization of a tetragonal insulator viewed as a lattice-valued object (lattice of solid dots). Solid (dashed) lines are at integer (half-integer) multiples of the quantum $e\mathbf{R}/V_{\text{cell}}$. Two possible "values" of $\mathbf{P}$ that respect inversion symmetry are shown in (a) and (b). Centrosymmetric $KNbO_3$ has polarization as in (b), while ferroelectrically polarized $KNbO_3$ corresponds to (c) (displacements exaggerated). Grey arrows in (c) indicate the possible assignments of "effective polarization," with the shorter one being the physical one in this case.

centrosymmetric $KNbO_3$ is non-zero. This is not likely to be a fruitful conversation! To provide a context-sensitive framework for discussing electric polarization, Resta and Vanderbilt (2007) introduced a distinction between two definitions of polarization:

- The *formal polarization* is defined by the Berry-phase theory, or in the classical context, by a formula like Eq. (1.18) or (4.59). It is intrinsically multivalued modulo a quantum $e\mathbf{R}/V_{\text{cell}}$.
- The *effective polarization* is instead defined to be the *change* in polarization relative to a nearby centrosymmetric[11] state.

The practicing computational theorist should be able to read and interpret the results of a calculation in the formal context, and then translate the results into the language of effective polarization for comparison with experiment and discussion with experimental colleagues.

In the case outlined above, the results for the formal polarizations of the centrosymmetric and up-domain states are $\{...,-51,51,...\}\,\mu\text{C/cm}^2$ and $\{...,-118,-16,86,...\}\,\mu\text{C/cm}^2$ respectively, so that ΔP should be chosen from the values $\{...,-67,+35,137,...\}\,\mu\text{C/cm}^2$. Since $35\,\mu\text{C/cm}^2$ is the smallest in magnitude, and the change is also in the expected direction, we can be reasonably confident that $+35\,\mu\text{C/cm}^2$ is the correct branch choice for ΔP_z. To provide more certainty, we try computing P_{nom} for the up-

[11] More precisely, the reference should be nonpolar. This does not necessarily require inversion symmetry; a counterexample is GaAs, where the tetrahedral symmetry is also sufficient.

domain state using the nominal ionic model of Eq. (4.59); suppose we find it to be $73\,\mu\mathrm{C/cm^2}$. Subtracting the previous value of $51\,\mu\mathrm{C/cm^2}$ we get $\Delta P_{\mathrm{nom}}{=}{+}22\,\mu\mathrm{C/cm^2}$, pointing to $+35\,\mu\mathrm{C/cm^2}$ as the closest value.[12] This is the value of effective polarization that we should focus on and report to our more practically-minded colleagues.

Of course, there is a potential problem with the definition of effective polarization: it has to be defined relative to a "nearby" nonpolar reference structure. The choice of this reference structure is usually obvious, but there can be exceptions. For example, $BiFeO_3$ is a perovskite ferroelectric that has been of considerable interest in recent years.[13] By averaging the atomic coordinates of $BiFeO_3$ over its two oppositely polarized configurations, we can arrrive at a centrosymmetric reference. Unfortunately, this reference structure is metallic, and so cannot be used to define a reference polarization. In such cases the safest approach is to consider carefully what is being measured experimentally. If the physical system exhibits a well-defined switching polarization, then the system must be following some kind of insulating path, and the theory should concentrate on identifying this path and computing the change of polarization along it.

4.4.3 Symmetry considerations

It is worth expanding briefly on the symmetry properties of lattice-valued quantities. For 3D systems in general, and 3D crystals in particular, one usually classifies physical properties as follows.

Ordinary scalars: The single value is invariant under spatial rotations.
Ordinary vectors: These transform according to the standard 3×3 rotation matrix $\mathcal{R}$.
Second-rank tensors: Each index of $A_{\mu\nu}$ is transformed by $\mathcal{R}$.
Symmetric second-rank tensors: Same as above but with $A_{\mu\nu} = A_{\nu\mu}$.
Antisymmetric second-rank tensors: Similar but with $A_{\mu\nu} = -A_{\nu\mu}$.

[12] Three comments are in order here. (i) Because of spin pairing, the electronic quantum is really $204\,\mu\mathrm{C/cm^2}$ in this example. If all calculations are done with a consistent choice of ionic cores, the lattice of possible ΔP values is really spaced by intervals of $204\,\mu\mathrm{C/cm^2}$, making the selection of $35\,\mu\mathrm{C/cm^2}$ rather obvious. (ii) The underestimate made by the nominal ionic model is related to the fact that the Born dynamical charges tend to be larger in magnitude than their nominal values in this class of transition-metal oxides. (iii) It may be tempting to inspect the individual changes of ionic and electronic polarization (Eqs. (4.51) and (4.50)) reported by the code, but this can be confusing because there are often large and opposite contributions in the two terms coming from included semicore shells, and as a result the branch choices made for the individual contributions are often rather arbitrary. The strategies described above are usually more productive.

[13] This interest derives in part from the fact that $BiFeO_3$ is also magnetic and has interesting couplings of electric, magnetic, and elastic properties.

And so on. (These quantities are often also assigned a prefix "pseudo" if there is an extra sign reversal under time reversal or improper spatial rotations.) In the crystalline context, for example, mass density is an ordinary scalar; magnetization is an ordinary (pseudo)vector; the delectric permittivity is a symmetric second-rank tensor; etc. (A quantity such as the magnetization, which may appear as a result of a symmetry-lowering phase transition, is often referred to as an "order parameter.") We now expand the list by including

Lattice-valued scalar: Its 1D lattice of values is spatially invariant.
Lattice-valued vector: Its lattice of vectors transforms according to $\mathcal{R}$.

The asynchronicity (see p. 130) is an example of the former, while the proper polarization $\mathbf{P}$ is an example of the latter.

Let's return briefly case of asynchronicity, which is an (admittedly somewhat contrived) example of a lattice-valued scalar. To briefly recap the scenario introduced on p. 130, we are listening to two clocks each ticking once per second, one loudly and one softly; the asynchronicity A is the time delay from a soft tick to a loud one. Suppose we make an audio recording and play it backwards; if we cannot tell the difference, then the physical situation respects time-reversal symmetry. What values of asynchronicity are consistent with time-reversal symmetry? A little reflection shows that there are *two* allowed values; the ticks can either be synchronized, $A = \{..., -1, 0, 1, ...\}$ s, or perfectly staggered, $A = \{..., -1/2, 1/2, ...\}$ s. Unlike the ordinary time difference $t_2 - t_1$ between two discrete events, there are now two "values" of A that are consistent with time-reversal symmetry.

In the context of crystal physics, the basic symmetry principle governing the allowed values of any of these quantities is that, if an operator $\mathcal{O}$ belongs to the crystal point group, then the quantity must have a value that transforms into itself under the action of $\mathcal{O}$. This principle applies equally to ordinary and lattice-valued quantities, but as for the asynchronicity example above, the symmetry-allowed possibilitis are typically more numerous for the lattice-valued quantities.

Let's return to the case of a centrosymmetric tetragonal crystal (cell dimensions $a \times a \times c$) with axis along $\hat{z}$. Let's also assume the point group includes inversion, the fourfold rotation C_4^z about the tetragonal axis, and other operations generated by these; this is the C_{4h} point group. If this crystal is ferromagnetic, its magnetization $\mathbf{M}$ must be of the form $M\hat{z}$, since any component in the x-y plane would not transform into itself under C_4^z. (Because magnetization is a pseudovector, its z component is not forced to vanish by inversion symmetry.) Its dielectric permittivity has to take the

form

$$\epsilon = \begin{pmatrix} u & 0 & 0 \\ 0 & u & 0 \\ 0 & 0 & v \end{pmatrix},$$

and so on. An ordinary vector quantity would be forced to vanish, but instead there are four (and only four) possibilites for the proper polarization $\mathbf{P}$ that are consistent with the C_{4h} point group. Since the quantum of polarization is $e\mathbf{R}/V_{\text{cell}}$, it is convenient to report these in the form $(V_{\text{cell}}/e)\mathbf{P}$. Then the four possibilities consistent with the point-group symmetry are $(V_{\text{cell}}/e)\mathbf{P} = \mathcal{L}_{(0,0,0)}$, $\mathcal{L}_{(a/2,a/2,0)}$, $\mathcal{L}_{(0,0,c/2)}$, and $\mathcal{L}_{(a/2,a/2,c/2)}$, where $\mathcal{L}_{\boldsymbol{\tau}}$ refers to the set of vectors $\mathbf{R} + \boldsymbol{\tau}$ where $\mathbf{R}$ runs over all lattice vectors. The first and last of these four possibilities are illustrated in Fig. 4.11(a-b) respectively.

The analysis becomes a little trickier to carry out for some other crystal symmetries, but the basic principles are the same. For example, consider the zincblende structure of GaAs. The lattice is face-centered cubic (fcc) with lattice vectors $\mathbf{a}_1 = (0, a/2, a/2)$, $\mathbf{a}_2 = (a/2, 0, a/2)$, and $\mathbf{a}_3 = (a/2, a/2, 0)$. We take the Ga to be at $\boldsymbol{\tau}_1 = (0, 0, 0)$ and the As at $\boldsymbol{\tau}_2 = (a/4, a/4, a/4)$. The point group is T_d, which is the full symmetry group of the tetrahedron including diagonal mirrors. The rescaled polarization lattice $(V_{\text{cell}}/e)\mathbf{P}$ is fcc, and the symmetry requires that it should either include the origin, or be symmetrically disposed about the origin. Here some investigation reveals that there are again four possibilities: $(V_{\text{cell}}/e)\mathbf{P} = \mathcal{L}_{(0,0,0)}$, $\mathcal{L}_{(a/2,a/2,a/2)}$ (which can also be written as $\mathcal{L}_{(a/2,0,0)}$), $\mathcal{L}_{(a/4,a/4,a/4)}$, and $\mathcal{L}_{(-a/4,-a/4,-a/4)}$.[14] A first-principles calculation confirms what we might guess, namely, that the formal polarization is the same as that of an ideal ionic model with ionic charges $+3e$ and $-3e$ on Ga and As atoms respectively.[15] This implies that the correct choice is $(V_{\text{cell}}/e)\mathbf{P} = \sum_s Z_s \boldsymbol{\tau}_s = (-3a/4, -3a/4, -3a/4)$, and using our freedom to translate by $\mathbf{R}$ we can write this as $(V_{\text{cell}}/e)\mathbf{P} = \mathcal{L}_{(a/4,a/4,a/4)}$. This is the correct result for the particular orientation of the GaAs crystal assumed above; applying a C_4^z or inversion operator to the GaAs crystal would change the result to $\mathcal{L}_{(-a/4,-a/4,-a/4)}$. However, no rotation or inver-

[14] Intuitively, these are connected with the high-symmetry sites in the unit cell of a simple fcc crystal such as Cu. These are the Cu site itself at $(0, 0, 0)$; the octahedral interstitial site at $(a/2, a/2, a/2)$; and the tetrahedral interstitial sites at $\pm(a/4, a/4, a/4)$. However, $(V_{\text{cell}}/e)\mathbf{P}$ should not be thought of as "located in" any physical unit cell. For example, $(V_{\text{cell}}/e)\mathbf{P}$ is independent of choice of origin, while the atomic coordinates are not. The quantity $(V_{\text{cell}}/e)\mathbf{P}$ just happens to have the same units and mathematical structure as a position in a unit cell.

[15] This can be rationalized in terms of the Wannier-center positions. A maximal localization procedure applied to GaAs gives four Wannier function, each of which lies on one of the four Ga-As bonds, but closer to the As than to the Ga. If we choose the Wannier centers to be the four lying close to the As atom at $(a/4, a/4, a/4)$, and recall that each carries charge $-2e$, we can group these together with the As core charge of $+5e$ to make a unit of net charge $-3e$ centered at the As position, leaving an ionic charge of $+3e$ on the Ga site.

sion of GaAs can access the other two symmetry-consistent values; these are simply not applicable to GaAs, but might apply to other insulating crystals having the same point group.

Note that we can convert wurtzite GaAs into diamond-structure Ge by moving a proton from the As nucleus at $(a/4, a/4, a/4)$ to the Ga nucleus at the origin. This changes the result to $\mathcal{L}_{(0,0,0)}$, as might be expected in view of the fact that the diamond structure is intrinsically non-polar.

The situation becomes even more complicated if we are motivated by spin degeneracy to try to keep track of the polarization modulo $2e\mathbf{R}/V_{\rm cell}$, instead of just modulo $e\mathbf{R}/V_{\rm cell}$. For a case like GaAs, where there are nuclei with odd-integer charges, a different choice of atomic basis (i.e., the set of chosen representative atoms $\boldsymbol{\tau}_j$ associated with the home unit cell) can shift $\mathbf{P}$ by half of this quantum. In this context, the correct symmetry principle is that a point-group operation acting on the polarization lattice must return it to itself, or to a one resulting from another valid choice of atomic basis. When only nuclei of even charge are present, we don't have to worry about that subtlety, but still the results can be surprising. For Si or Ge, for example, the polarization is given by Eq. (4.55) with ionic charges $+4e$ at the atomic sites and $-2e$ at each of the four midbond positions, so that $\sum_s Z_s \boldsymbol{\tau}_s - \sum_n \bar{\mathbf{r}}_n = (-a, -a, -a)$. The result is that $(V_{\rm cell}/2e)\mathbf{P} = \mathcal{L}_{(a/2,a/2,a/2)}$. So, with spin degeneracy taken into account, the formal polarization does not vanish even for Si or Ge!

The interested reader can find some further discussion of these symmetry considerations in Sec. III.E of Vanderbilt and King-Smith (1993). From the perspective of a practitioner of first-principles calculations, however, the main thing to keep in mind is that a non-zero formal polarization in a high-symmetry structure is not necessarily a sign that anything is amiss. If you focus instead on computing changes in formal polarization with respect to a high-symmetry reference structure,[16] i.e., the effective polarization, then it should not be necessary to delve deeply into these symmetry considerations.

Exercise 4.4.1 Show...

4.5 Surface charge theorem

Exercise 4.5.1 Show...

[16] Here "high symmetry" means that an ordinary vector order parameter is forced to vanish.

4.6 Uniform electric fields

Exercise 4.6.1 Show...